hep-ph/0412147

Two-loop gluino contributions to neutron electric dipole moment in CP violating MSSM

Tai-Fu Feng[a], Xue-Qian Li[b,c], Jukka Maalampi[a], Xinmin Zhang[c]

[a] *Department of Physics, 40014 University of Jyväskylä,Finland*

[b] *Department of Physics, Nankai University,*

Tianjing 300071, P. R. China and

[c] *Institute of High Energy Physics, Academy of Science of China,*

P.O. Box 918, Beijing 100039, P. R. China

(Dated: February 2, 2008)

Abstract

We analyze two-loop gluino corrections to the neutron electric dipole moment (EDM) in the minimal supersymmetry extension of the standard model (MSSM). The dependence of two-loop corrections on the relevant CP violating phases differs from that of the one-loop contributions, and there is a region in the parameter space where the two-loop contributions are comparable with the one-loop contributions. Our numerical results show that the two-loop corrections can be as large as 30% of the one-loop results.

PACS numbers: 11.30.Er, 12.60.Jv,14.80.Cp

Keywords: two-loop, electric dipole moment, supersymmetry

I. INTRODUCTION

The fermion electric dipole moments (EDMs) offer a powerful probe for new physics beyond the Standard Model (SM). In the SM, the EDM of the neutron is fully induced by the CP phase of the Cabibbo-Kobayashi-Maskawa (CKM) matrix elements and it is predicted to be much smaller [1] than the present experimental upper limit of $1.1 \times 10^{-25}\ e \cdot cm$ [2] and beyond the reach of experiment in the near future. As for the minimal supersymmetric extension of the SM (MSSM), there are many new sources of the CP violation that can result in larger contributions to the EDM of the neutron [3, 4]. Taking the CP phases with a natural size of $\mathcal{O}(1)$, and the supersymmetry mass spectra at the TeV range, the theoretical prediction on the neutron EDM at one-loop level already exceeds the present experimental upper bound. In order to make the theoretical prediction consistent with the experimental data, three approaches are adopted in the literature. One possibility is to make the CP phases sufficiently small, i.e. $\leq 10^{-2}$ [3]. One can also assume a mass suppression by making the supersymmetry spectra heavy, i.e. in the several TeV range [4], or invoke a cancellation among the different contributions to the fermion EDMs [5].

The prediction for the fermion EDMs at one-loop level in a supersymmetric theory has been extensively discussed in the literature. On other hand, the analysis on the neutron EDM at two-loop level is less advanced, even though some pioneer work has been carried out, for example the two-loop Barr-Zee type diagrams involving the Higgs bosons [6] and the purely gluonic dimension-six Weinberg operator induced by two-loop gluino-squark diagrams [7] have been analyzed.

Analyzing the EDMs at two-loop order can give us a better understanding of where the new physics scale may emerge and shed some light to the spectra of new physical particles around this scale. Moreover, the two-loop analysis involves some new parameters in addition to those appearing in the one-loop calculations, hence resulting in more rigorous constraints on the supersymmetry parameter space.

In this work we shall analyse the two-loop gluino corrections to the neutron EDM in the MSSM. We work in the framework of the simplest model, where we will neglect all other possible sources of flavor violation except those related to the CKM matrix, and try to avoid ambiguities of the unification conditions of the soft-breaking parameters at the grand unification scale present in the mSUGRA schemes. In the next Section, we will demonstrate

how to obtain the two-loop gluino corrections to the neutron EDM. In the Section III we will present the results of our numerical computations and we study the dependence of the neutron EDM on the supersymmetry parameters. Conclusions are presented in Section IV.

II. THE TWO-LOOP GLUINO CORRECTIONS TO THE NEUTRON EDM

In the effective Lagrangian, the fermion EDM d_f is defined through the dimension five operator

$$\mathcal{L}_{EDM} = -\frac{i}{2} d_f \overline{f} \sigma^{\mu\nu} \gamma_5 f F_{\mu\nu} \tag{1}$$

where$f$ is a fermion field, $F_{\mu\nu}$ is the electromagnetic field strength. This coupling obviously signifies a CP violation. It is not present among the fundamental interactions at tree level, but it is generated in loop level in an electroweak theory with CP violation. Moreover, because quarks also take part in strong interactions, the chromoelectric dipole moment (CEDM) $\overline{f} T^a \sigma^{\mu\nu} \gamma_5 f G^a_{\mu\nu}$ of quarks, where T^a ($a = 1, \cdots, 8$) denote the generators of the strong $SU(3)$ gauge group, $G^a_{\mu\nu}$ is the gluon field strength, and the pure gluon Weinberg operator of dimension-six, $f_{abc} G^a_{\mu\rho} G^{b\rho}_{\nu} G^c_{\lambda\sigma} \epsilon^{\mu\nu\lambda\sigma}$, contributes to the quark EDMs as well.

A convenient way to describe loop-induced contributions is the effective theory approach, where the heavy particles are integrated out at the matching scale. The resulting effective Lagrangian includes a full set of CP violation operators. In this work, we restrict ourselves to the following operators that are relevant to the neutron EDM:

$$\mathcal{L}_{eff} = \sum_{i}^{5} C_i(\Lambda) \mathcal{Q}_i(\Lambda) \ , \tag{2}$$

where $C_i(\Lambda)$ are the Wilson coefficients evaluated at the scale Λ, and the five operators of interests are

$$\begin{aligned}
\mathcal{Q}_1 &= \overline{q} \sigma^{\mu\nu} \omega_- q F_{\mu\nu} \ , \\
\mathcal{Q}_2 &= \overline{q} \sigma^{\mu\nu} \omega_+ q F_{\mu\nu} \ , \\
\mathcal{Q}_3 &= \overline{q} T^a \sigma^{\mu\nu} \omega_- q G^a_{\mu\nu} \ , \\
\mathcal{Q}_4 &= \overline{q} T^a \sigma^{\mu\nu} \omega_+ q G^a_{\mu\nu} \ , \\
\mathcal{Q}_5 &= -\frac{1}{6} f_{abc} G^a_{\mu\rho} G^{b\rho}_{\nu} G^c_{\lambda\sigma} \epsilon^{\mu\nu\lambda\sigma} \ .
\end{aligned} \tag{3}$$

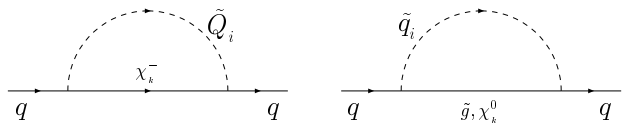

FIG. 1: The one-loop self energy diagrams which lead to the quark EDMs and CEDMs in MSSM, the corresponding triangle diagrams are obtained by attaching a photon or a gluon in all possible ways to the SUSY particles.

The effective triangle diagrams responsible for the quark EDMs and CEDMs, are obtained by attaching a photon or gluon external line,for quark EDM or CEDM, respectively, in all possible ways to the quark self-energy diagrams.

The one-loop supersymmetric corrections to the Wilson coefficients $C_i(\Lambda)$ in Eq. (2) originate from three types of the graphs: the quark self-energy diagrams, where one has a gluino and a squark, a chargino and a squark or a neutralino and a squark as virtual particles in the loop (Fig.1). We will adopt below a terminology where, for example, the "gluino-squark contribution" means the sum of those triangle diagrams, which have a gluino and a squark as virtual states and where a photon or a gluon in attached in all possible ways to the external line.

Before moving to derive the two-loop gluino corrections, we first present, in order to familiarize our notation, the one-loop results. Those expressions can be found in the literature, and we just translate them here into our notations for later convenience.

The corrections from the gluino-squark diagrams are

$$
\begin{aligned}
d^{\gamma}_{\tilde{g}(1)} &= -\frac{2}{3\pi} e_q e \alpha_s \sum_{i=1}^{2} \mathbf{Im}\Big((\mathcal{Z}_{\tilde{q}})_{2,i} (\mathcal{Z}^{\dagger}_{\tilde{q}})_{i,1} e^{-i\theta_3} \Big) \\
&\quad \times \frac{|m_{\tilde{g}}|}{m^2_{\tilde{q}_i}} B\Big(\frac{|m_{\tilde{g}}|^2}{m^2_{\tilde{q}_i}} \Big) \, , \\
d^{g}_{\tilde{g}(1)} &= \frac{g_3 \alpha_s}{4\pi} \sum_{i=1}^{2} \mathbf{Im}\Big((\mathcal{Z}_{\tilde{q}})_{2,i} (\mathcal{Z}^{\dagger}_{\tilde{q}})_{i,1} e^{-i\theta_3} \Big) \\
&\quad \times \frac{|m_{\tilde{g}}|}{m^2_{\tilde{q}_i}} C\Big(\frac{|m_{\tilde{g}}|^2}{m^2_{\tilde{q}_i}} \Big) \, .
\end{aligned}
\tag{4}
$$

Here $\alpha_s = g_3^2/(4\pi)$, θ_3 denotes the phase of the soft gluino mass $m_{\tilde{g}}$, and $\mathcal{Z}_{\tilde{q}}$ are the mixing matrices of the squarks, i.e. $\mathcal{Z}^{\dagger}_{\tilde{q}} \mathbf{m}^2_{\tilde{q}} \mathcal{Z}_{\tilde{q}} = diag(m^2_{\tilde{q}_1}, \, m^2_{\tilde{q}_2})$ where

$$\mathbf{m}^2_{\tilde{q}} = \begin{pmatrix} m^2_{\tilde{Q}} + m^2_q + m^2_z(\frac{1}{2} - Q_q s^2_{\rm w})\cos 2\beta & m_q(A^*_q - \mu R_q) \\ m_q(A_q - \mu^* R_q) & m^2_{\{\tilde{U},\tilde{D}\}} + m^2_q + m^2_z(\frac{1}{2} - Q_q s^2_{\rm w})\cos 2\beta \end{pmatrix} , \quad (5)$$

with $Q_q = 2/3(-1/3)$, $R_q = \tan\beta(1/\tan\beta)$ for $q = u$ (d). As usual, $\tan\beta = v_u/v_d$ is the ratio between the VEVs of the up- and down-type Higgs fields, and $\theta_{\rm W}$ is the weak mixing angle. We also use the short-hand notations $s_{\rm W} = \sin\theta_{\rm W}$, $c_{\rm W} = \cos\theta_{\rm W}$. The loop functions $B(r)$ and $C(r)$ are defined as $B(r) = [2(r-1)^2]^{-1}[1 + r + 2r\ln r/(r-1)]$ and $C(r) = [6(r-1)^2]^{-1}[10r - 26 - (2r-18)\ln r/(r-1)]$.

In a similar way, the one-loop neutralino-squark contributions can be written as

$$\begin{aligned} d^{\gamma}_{\chi^0_k(1)} &= e_q \frac{e\alpha}{16\pi s^2_{\rm w} c^2_{\rm w}} \sum_{i,k} \mathbf{Im}\Big((A^q_N)_{k,i}(B^q_N)^{\dagger}_{i,k}\Big) \\ &\quad \times \frac{m_{\chi^0_k}}{m^2_{\tilde{q}_i}} B\Big(\frac{m^2_{\chi^0_k}}{m^2_{\tilde{q}_i}}\Big) , \\ d^{g}_{\chi^0_k(1)} &= \frac{g_3\alpha_s}{64\pi s^2_{\rm w} c^2_{\rm w}} \sum_{i,k} \mathbf{Im}\Big((A^q_N)_{k,i}(B^q_N)^{\dagger}_{i,k}\Big) \\ &\quad \times \frac{m_{\chi^0_k}}{m^2_{\tilde{q}_i}} B\Big(\frac{m^2_{\chi^0_k}}{m^2_{\tilde{q}_i}}\Big) \end{aligned} \quad (6)$$

with

$$\begin{aligned} (A^u_N)_{k,i} &= -\frac{4}{3} s_{\rm w} (\mathcal{Z}_{\tilde{u}})_{2,i} (\mathcal{Z}_N)_{1,k} + \frac{m_u c_{\rm w}}{m_{\rm w} s_\beta} \\ &\quad \times (\mathcal{Z}_{\tilde{u}})_{1,i} (\mathcal{Z}_N)_{4,k} , \\ (B^u_N)_{k,i} &= (\mathcal{Z}_{\tilde{u}})_{1,i} \Big(\frac{s_{\rm w}}{3} (\mathcal{Z}_N)^*_{1,k} + c_{\rm w} (\mathcal{Z}_N)^*_{2,k}\Big) \\ &\quad + \frac{m_u c_{\rm w}}{m_{\rm w} s_\beta} (\mathcal{Z}_{\tilde{u}})_{2,i} (\mathcal{Z}_N)^*_{4,k} , \\ (A^d_N)_{k,i} &= \frac{2}{3} s_{\rm w} (\mathcal{Z}_{\tilde{d}})_{2,i} (\mathcal{Z}_N)_{1,k} + \frac{m_d c_{\rm w}}{m_{\rm w} c_\beta} \\ &\quad \times (\mathcal{Z}_{\tilde{d}})_{1,i} (\mathcal{Z}_N)_{3,k} , \\ (B^d_N)_{k,i} &= (\mathcal{Z}_{\tilde{d}})_{1,i} \Big(\frac{s_{\rm w}}{3} (\mathcal{Z}_N)^*_{1,k} - c_{\rm w} (\mathcal{Z}_N)^*_{2,k}\Big) \\ &\quad + \frac{m_d c_{\rm w}}{m_{\rm w} c_\beta} (\mathcal{Z}_{\tilde{d}})_{2,i} (\mathcal{Z}_N)^*_{3,k} . \end{aligned} \quad (7)$$

Here $\alpha = e^2/(4\pi)$, $s_\beta = \sin\beta$, $c_\beta = \cos\beta$, $m_{\chi^0_k}$ $(k = 1,\ 2,\ 3,\ 4)$ denote the eigenvalues of neutralino mass matrix, and $\mathcal{Z}_N$ is the correspondingly mixing matrix.

Finally, the chargino-squark contributions are given by

$$
\begin{aligned}
d^{\gamma}_{\chi^{\pm}_k(1)} &= \frac{e\alpha}{4\pi s_{\rm w}^2} V^{\dagger}_{qQ} V_{Qq} \sum_{i,k} \mathbf{Im}\Big((A^Q_C)_{k,i} (B^Q_C)^{\dagger}_{i,k} \Big) \frac{m_{\chi^{\pm}_k}}{m^2_{\tilde{Q}_i}} \\
&\quad \times \Big[e_{_Q} B\Big(\frac{m^2_{\chi^{\pm}_k}}{m^2_{\tilde{Q}_i}} \Big) + (e_{_q} - e_{_Q}) A\Big(\frac{m^2_{\chi^{\pm}_k}}{m^2_{\tilde{Q}_i}} \Big) \Big] \ , \\
d^{g}_{\chi^{\pm}_k(1)} &= \frac{g_3\alpha}{4\pi s_{\rm w}^2} V^{\dagger}_{qQ} V_{Qq} \sum_{i,k} \mathbf{Im}\Big((A^Q_C)_{k,i} (B^Q_C)^{\dagger}_{i,k} \Big) \\
&\quad \times \frac{m_{\chi^{\pm}_k}}{m^2_{\tilde{Q}_i}} B\Big(\frac{m^2_{\chi^{\pm}_k}}{m^2_{\tilde{Q}_i}} \Big) \ ,
\end{aligned}
\tag{8}
$$

where V denotes the CKM matrix, $m_{\chi^{\pm}_k}$ $(k = 1,\ 2)$ are the masses of charginos, and the loop function $A(r) = 2(1-r)^{-2}[3 - r + 2\ln r/(1-r)]$. The couplings appearing in these expressions are defined as

$$
\begin{aligned}
(A^d_C)_{k,i} &= \frac{m_{_u}}{\sqrt{2} m_{\rm w} s_{_\beta}} (\mathcal{Z}_{\tilde{d}})_{1,i} (\mathcal{Z}_{+})_{2,k} \ , \\
(B^d_C)_{k,i} &= \frac{m_{_d}}{\sqrt{2} m_{\rm w} c_{_\beta}} (\mathcal{Z}_{\tilde{d}})_{2,i} (\mathcal{Z}_{-})_{2,k} - (\mathcal{Z}_{\tilde{d}})_{1,i} (\mathcal{Z}_{-})_{1,k} \ ,
\end{aligned}
$$

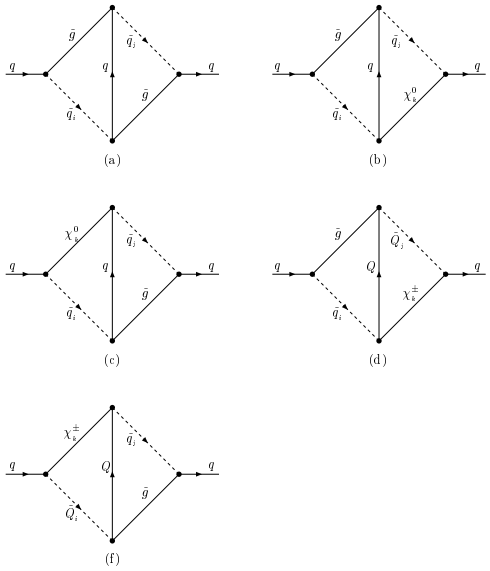

FIG. 2: The two-loop self energy diagrams which lead to the quark EDMs and CEDMs in the MSSM, the corresponding triangle diagrams are obtained by attaching a photon or gluon in all possible ways to the SUSY particles.

$$
\begin{aligned}
(A^u_{C})_{k,i} &= \frac{m_{_d}}{\sqrt{2} m_{_{\rm w}} c_{_\beta}} (\mathcal{Z}_{_{\tilde{u}}})_{1,i} (\mathcal{Z}_{_-})^*_{2,k} \ , \\
(B^u_{C})_{k,i} &= \frac{m_{_u}}{\sqrt{2} m_{_{\rm w}} s_{_\beta}} (\mathcal{Z}_{_{\tilde{u}}})_{2,i} (\mathcal{Z}_{_+})^*_{2,k} - (\mathcal{Z}_{_{\tilde{u}}})_{1,i} (\mathcal{Z}_{_+})^*_{1,k} \ ,
\end{aligned}
\tag{9}
$$

where $\mathcal{Z}_{_+}$ and $\mathcal{Z}_{_-}$ are the right- and left-handed mixing matrices of the charginos, respectively. It is noteworthy that one-loop chargino corrections to the quark EDMs and CEDMs are proportional to the suppression factors $m_{_q}/m_{_{\rm w}}$ contained in the couplings A^q_{C} $(q = u,\ d)$.

The two-loop gluino corrections to the Wilson coefficients originate from the two-loop self-energy diagrams for quarks, depicted in Fig. 2. The corresponding dipole moment diagrams are obtained by attaching a photon or gluon to these diagrams in all possible ways. In these diagrams there is no new suppression factor, except a factor arising from loop integration, and the divergence caused by the sub-diagrams is subtracted in $\overline{MS}$ scheme safely. It turns out that for some region of the parameter space the two-loop results are comparable with the one-loop contributions. The reason for this is that the dependence of the two-loop results on the relevant CP phases differs from that of the one-loop results.

Since the two-loop analysis is more subtle than the analysis at one-loop level, we present here in some detail all the processes, which contribute at two-loop level into the theoretical prediction of the quark EDMs. Taking the same steps, which we did in our earlier works [8], we obtain the following expression for the relevant effective Lagrangian:

$$
\begin{aligned}
\mathcal{L}^{\tilde{g}\tilde{g}}_{_{eff}} = \frac{4}{9} g_3^4 \int \frac{d^D q_1}{(2\pi)^D} \frac{d^D q_2}{(2\pi)^D} \frac{1}{\mathcal{D}_{_{\tilde{g}}}} \\
\times \Big\{ (\mathcal{Z}_{_{\tilde{q}}})_{2,j} (\mathcal{Z}^\dagger_{_{\tilde{q}}})_{j,1} (\mathcal{Z}_{_{\tilde{q}}})_{1,i} (\mathcal{Z}^\dagger_{_{\tilde{q}}})_{i,1} |m_{_{\tilde{g}}}| e^{-i\theta_3} \Big[e_{_q} e \mathcal{N}^{\gamma}_{_{\tilde{g}(1)}} \mathcal{Q}_1 + g_3 \mathcal{N}^{g}_{_{\tilde{g}(1)}} \mathcal{Q}_3 \Big] \\
+ (\mathcal{Z}_{_{\tilde{q}}})_{1,j} (\mathcal{Z}^\dagger_{_{\tilde{q}}})_{j,2} (\mathcal{Z}_{_{\tilde{q}}})_{2,i} (\mathcal{Z}^\dagger_{_{\tilde{q}}})_{i,2} |m_{_{\tilde{g}}}| e^{i\theta_3} \Big[e_{_q} e \mathcal{N}^{\gamma}_{_{\tilde{g}(1)}} \mathcal{Q}_2 + g_3 \mathcal{N}^{g}_{_{\tilde{g}(1)}} \mathcal{Q}_4 \Big] \\
+ (\mathcal{Z}_{_{\tilde{q}}})_{2,j} (\mathcal{Z}^\dagger_{_{\tilde{q}}})_{j,2} (\mathcal{Z}_{_{\tilde{q}}})_{2,i} (\mathcal{Z}^\dagger_{_{\tilde{q}}})_{i,1} |m_{_{\tilde{g}}}| e^{-i\theta_3} \Big[e_{_q} e \mathcal{N}^{\gamma}_{_{\tilde{g}(2)}} \mathcal{Q}_1 + g_3 \mathcal{N}^{g}_{_{\tilde{g}(2)}} \mathcal{Q}_3 \Big] \\
+ (\mathcal{Z}_{_{\tilde{q}}})_{1,j} (\mathcal{Z}^\dagger_{_{\tilde{q}}})_{j,1} (\mathcal{Z}_{_{\tilde{q}}})_{1,i} (\mathcal{Z}^\dagger_{_{\tilde{q}}})_{i,2} |m_{_{\tilde{g}}}| e^{i\theta_3} \Big[e_{_q} e \mathcal{N}^{\gamma}_{_{\tilde{g}(2)}} \mathcal{Q}_2 + g_3 \mathcal{N}^{g}_{_{\tilde{g}(2)}} \mathcal{Q}_4 \Big] \Big\} + \cdots \ ,
\end{aligned}
\tag{10}
$$

where $\mathcal{D}_{_{\tilde{g}}} = ((q_2 - q_1)^2 - m_q^2)(q_1^2 - |m_{_{\tilde{g}}}|^2)(q_1^2 - m^2_{_{\tilde{q}_j}})(q_2^2 - m^2_{_{\tilde{q}_i}})(q_2^2 - |m_{_{\tilde{g}}}|^2)$ and D is the time-space dimension. We collect the complicated form factor $\mathcal{N}_{_{\tilde{g}}}$ in appendix A.

The effective Lagrangian of Eq. (10) originates in fact from the contributions of the effective triangle vertices induced by the "gluino-gluino self-energy" (Fig.2 (a)). The terminology here is analogous to the one adopted in the one-loop case above. The gluino-gluino self-energy is a short-hand expression for a diagram, where we attach a photon or gluon line

in all possible ways to the two-loop quark self-energy diagram having, besides the squark, two gluinos are as intermediate agents. Because the sum of the triangle diagrams corresponding to each "self-energy" obviously respects the gauge invariance, we can calculate the contributions of all the "self-energies" separately. We will use below the following identities demanded by the translational invariance of the loop-momenta:

$$\begin{aligned}
&\int \frac{d^Dq_1}{(2\pi)^D}\frac{d^Dq_2}{(2\pi)^D}\frac{1}{\mathcal{D}_{_0}}\Big\{-\frac{2+D}{D}q_1\cdot(q_2-q_1)\\
&+\frac{2}{q_2^2-m_{_2}^2}\Big[\frac{D(q_1\cdot q_2)^2-q_1^2q_2^2}{D(D-1)}-\frac{q_1^2q_1\cdot q_2}{D}\Big]\\
&+\frac{2}{q_1^2-m_{_1}^2}\frac{q_1^2q_1\cdot(q_2-q_1)}{D}\Big\}\equiv 0\,,\\
&\int \frac{d^Dq_1}{(2\pi)^D}\frac{d^Dq_2}{(2\pi)^D}\frac{1}{\mathcal{D}_{_0}}\Big\{-q_1\cdot(q_2-q_1)\\
&+\frac{2}{q_1^2-m_{_1}^2}\Big[\frac{D(q_1\cdot q_2)^2-q_1^2q_2^2}{D(D-1)}-\frac{q_1^2q_1\cdot q_2}{D}\Big]\\
&+\frac{2}{q_2^2-m_{_2}^2}\frac{q_1\cdot(q_2-q_1)q_2^2}{D}\Big\}\equiv 0\,,
\end{aligned}\tag{11}$$

where $\mathcal{D}_{_0}=((q_2-q_1)^2-m_{_0}^2)(q_1^2-m_{_1}^2)(q_2^2-m_{_2}^2)$. We find

$$\begin{aligned}
&\int \frac{d^Dq_1}{(2\pi)^D}\frac{d^Dq_2}{(2\pi)^D}\frac{\mathcal{N}^{\gamma}_{\tilde g(2)}}{\mathcal{D}_{\tilde g}}\big(\tilde q_i\leftrightarrow\tilde q_j,\ q_1\leftrightarrow q_2\big)\\
=\ &\int \frac{d^Dq_1}{(2\pi)^D}\frac{d^Dq_2}{(2\pi)^D}\frac{1}{\mathcal{D}_{\tilde g}}\Big\{\frac{2}{D}\frac{q_1\cdot(q_1-q_2)}{q_1^2-m_{\tilde q_j}^2}+\frac{4}{D}\frac{q_2^2q_1\cdot(q_1-q_2)}{(q_2^2-m_{\tilde q_i}^2)^2}-\frac{q_1\cdot(q_1-q_2)}{q_2^2-m_{\tilde q_i}^2}\\
&+\frac{4}{(q_2^2-m_{\tilde q_i}^2)(q_1^2-|m_{\tilde g}|^2)}\Big[\frac{q_1\cdot q_2q_1^2}{D}-\frac{D(q_1\cdot q_2)^2-q_1^2q_2^2}{D(D-1)}\Big]+\frac{4}{D}\frac{q_1^2q_1\cdot(q_1-q_2)}{(q_1^2-|m_{\tilde g}|^2)^2}\\
&-\frac{2+D}{D}\frac{q_1\cdot(q_1-q_2)}{q_1^2-|m_{\tilde g}|^2}+\frac{2-D}{D}\frac{q_1\cdot(q_1-q_2)}{(q_2-q_1)^2-m_{_q}^2}\Big\}\\
=\ &\int \frac{d^Dq_1}{(2\pi)^D}\frac{d^Dq_2}{(2\pi)^D}\frac{1}{\mathcal{D}_{\tilde g}}\Big\{\frac{D-2}{D}\frac{q_1\cdot(q_2-q_1)}{(q_2-q_1)^2-m_{_q}^2}+\frac{2}{D}\frac{q_1^2q_1\cdot(q_2-q_1)}{(q_1^2-|m_{\tilde g}|^2)(q_1^2-m_{\tilde q_j}^2)}\\
&+\Big[\frac{2}{(q_1^2-|m_{\tilde g}|^2)(q_2^2-|m_{\tilde g}|^2)}+\frac{1}{(q_1^2-m_{\tilde q_j}^2)(q_2^2-m_{\tilde q_i}^2)}\Big]\Big[\frac{D(q_1\cdot q_2)^2-q_1^2q_2^2}{D(D-1)}\\
&-\frac{q_1^2q_1\cdot q_2}{D}\Big]+\frac{2}{D}\frac{q_2^2q_1\cdot(q_2-q_1)}{(q_2^2-m_{\tilde q_i}^2)(q_2^2-|m_{\tilde g}|^2)}-\frac{2}{D}\frac{q_1\cdot(q_2-q_1)}{q_1^2-m_{\tilde q_j}^2}\Big\}\\
=\ &\int \frac{d^Dq_1}{(2\pi)^D}\frac{d^Dq_2}{(2\pi)^D}\frac{1}{\mathcal{D}_{\tilde g}}\Big\{\frac{D-2}{D}\frac{q_1\cdot(q_2-q_1)}{(q_2-q_1)^2-m_{_q}^2}-\frac{4}{D}\frac{q_1\cdot(q_2-q_1)q_2^2}{(q_2^2-|m_{\tilde g}|^2)^2}\\
&-\frac{4}{(q_1^2-m_{\tilde q_j}^2)(q_2^2-|m_{\tilde g}|^2)}\Big[\frac{D(q_1\cdot q_2)^2-q_1^2q_2^2}{D(D-1)}-\frac{q_1^2q_1\cdot q_2}{D}\Big]
\end{aligned}$$

$$
\begin{aligned}
&-\frac{4}{D}\frac{q_1^2 q_1\cdot(q_2-q_1)}{(q_1^2-m_{\tilde{q}_j}^2)^2}+\frac{q_1\cdot(q_2-q_1)}{q_2^2-|m_{\tilde{g}}|^2}+\frac{q_1\cdot(q_2-q_1)}{q_1^2-m_{\tilde{q}_j}^2}\Big\}\\
=&\quad\int\frac{d^Dq_1}{(2\pi)^D}\frac{d^Dq_2}{(2\pi)^D}\frac{\mathcal{N}^{\gamma}_{\tilde{g}(1)}}{\mathcal{D}_{\tilde{g}}}\,. \qquad (12)
\end{aligned}
$$

Similarly, we find

$$
\begin{aligned}
&\int\frac{d^Dq_1}{(2\pi)^D}\frac{d^Dq_2}{(2\pi)^D}\frac{\mathcal{N}^{g}_{\tilde{g}(2)}}{\mathcal{D}_{\tilde{g}}}\Big(\tilde{q}_i\leftrightarrow\tilde{q}_j,\ q_1\leftrightarrow q_2\Big)\\
=&\quad\int\frac{d^Dq_1}{(2\pi)^D}\frac{d^Dq_2}{(2\pi)^D}\frac{\mathcal{N}^{g}_{\tilde{g}(1)}}{\mathcal{D}_{\tilde{g}}}\,. \qquad (13)
\end{aligned}
$$

With the help of Eq.(12) and Eq.(13), the corresponding terms in Eq.(10) are transformed into

$$
\begin{aligned}
\mathcal{L}^{\tilde{g}\tilde{g}}_{eff}=&-i\frac{4}{9}e_{_q}eg_3^4|m_{\tilde{g}}|\int\frac{d^Dq_1}{(2\pi)^D}\frac{d^Dq_2}{(2\pi)^D}\frac{\mathcal{N}^{\gamma}_{\tilde{g}(1)}}{\mathcal{D}_{\tilde{g}}}\mathbf{Im}\Big((\mathcal{Z}_{\tilde{q}})_{2,j}(\mathcal{Z}^{\dagger}_{\tilde{q}})_{j,1}e^{-i\theta_3}\Big)\cdot\Big[\bar{q}\sigma^{\mu\nu}\gamma_5 qF_{\mu\nu}\Big]\\
&-i\frac{4}{9}g_3^5|m_{\tilde{g}}|\int\frac{d^Dq_1}{(2\pi)^D}\frac{d^Dq_2}{(2\pi)^D}\frac{\mathcal{N}^{g}_{\tilde{g}(1)}}{\mathcal{D}_{\tilde{g}}}\mathbf{Im}\Big((\mathcal{Z}_{\tilde{q}})_{2,j}(\mathcal{Z}^{\dagger}_{\tilde{q}})_{j,1}e^{-i\theta_3}\Big)\cdot\Big[\bar{q}T^a\sigma^{\mu\nu}\gamma_5 qG^a_{\mu\nu}\Big]\\
&+\cdots\,. \qquad (14)
\end{aligned}
$$

The two-loop scalar integrations can be reduced into the two-loop vacuum integrals defined as

$$
\int\frac{d^Dq_1d^Dq_2}{(q_1-q_2)^2-m_0^2)(q_1^2-m_1^2)(q_2^2-m_2^2)},
$$

which was analyzed in detail [9]. However, the two-loop scalar integration $\int\frac{d^Dq_1}{(2\pi)^D}\frac{d^Dq_2}{(2\pi)^D}\frac{\mathcal{N}^{\gamma,g}_{\tilde{g}(1)}}{\mathcal{D}_{\tilde{g}}}$ contain the ultra-violet divergence which originates from the sub-daigrams. After the renormalization in $\overline{MS}$ scheme, we finally obtain the corrections from the two-loop "gluino-gluino" diagram to the quark EDMs and CEDMs respectively as

$$
\begin{aligned}
d^{\gamma}_{\tilde{g}(2)}&=\frac{8e_{_q}e\alpha_s^2|m_{\tilde{g}}|}{9(4\pi)^2m_{_{\rm w}}^2}F_1(x_{_q},x_{\tilde{q}_j},x_{\tilde{g}},x_{\tilde{g}},x_{\tilde{q}_i})\mathbf{Im}\Big((\mathcal{Z}_{\tilde{q}})_{2,j}(\mathcal{Z}^{\dagger}_{\tilde{q}})_{j,1}e^{-i\theta_3}\Big)\,,\\
d^{g}_{\tilde{g}(2)}&=\frac{8g_3\alpha_s^2|m_{\tilde{g}}|}{9(4\pi)^2m_{_{\rm w}}^2}F_3(x_{_q},x_{\tilde{q}_j},x_{\tilde{g}},x_{\tilde{g}},x_{\tilde{q}_i})\mathbf{Im}\Big((\mathcal{Z}_{\tilde{q}})_{2,j}(\mathcal{Z}^{\dagger}_{\tilde{q}})_{j,1}e^{-i\theta_3}\Big)\,, \qquad (15)
\end{aligned}
$$

with $x_i=m_i^2/m_{_{\rm w}}^2$, and the function $F_i(x_0,x_1,x_2,x_3,x_4)$ $(i=1,\ 3)$ are defined in appendix B.

The effective Lagrangian, which corresponds to the contributions of the triangle diagrams induced in the "neutralino-gluino" self-energy (i.e. diagrams where loop squarks are

accompanied with neutralinos and gluinos, see Fig.2 (b) and (c)), includes the following pieces:

$$
\begin{aligned}
\mathcal{L}_{eff}^{\tilde{g}\chi_k^0} = & \frac{2}{3}\frac{e^2 g_3^2}{s_{\rm w}^2 c_{\rm w}^2}\int\frac{d^Dq_1}{(2\pi)^D}\frac{d^Dq_2}{(2\pi)^D}\frac{1}{\mathcal{D}^{(a)}_{\chi_k^0}} \\
& \times\Big\{(A_N^q)_{kj}(\mathcal{Z}_{\tilde{q}}^\dagger)_{j,1}(B_N^q)_{ki}(\mathcal{Z}_{\tilde{q}}^\dagger)_{i,1}|m_{\tilde{g}}|e^{-i\theta_3}\Big[e_q e\mathcal{N}^{\gamma}_{\tilde{g}(1)}\mathcal{Q}_1+g_3\mathcal{N}^{g(a)}_{\chi_k^0(1)}\mathcal{Q}_3\Big] \\
& +(B_N^q)_{kj}(\mathcal{Z}_{\tilde{q}}^\dagger)_{j,2}(A_N^q)_{ki}(\mathcal{Z}_{\tilde{q}}^\dagger)_{i,2}|m_{\tilde{g}}|e^{i\theta_3}\Big[e_q e\mathcal{N}^{\gamma}_{\tilde{g}(1)}\mathcal{Q}_2+g_3\mathcal{N}^{g(a)}_{\chi_k^0(1)}\mathcal{Q}_4\Big] \\
& -(A_N^q)_{kj}(\mathcal{Z}_{\tilde{q}}^\dagger)_{j,2}(A_N^q)_{ki}(\mathcal{Z}_{\tilde{q}}^\dagger)_{i,1}m_{\chi_k^0}\Big[e_q e\mathcal{N}^{\gamma}_{\tilde{g}(2)}\mathcal{Q}_1+g_3\mathcal{N}^{g(a)}_{\chi_k^0(2)}\mathcal{Q}_3\Big] \\
& -(B_N^q)_{kj}(\mathcal{Z}_{\tilde{q}}^\dagger)_{j,1}(B_N^q)_{ki}(\mathcal{Z}_{\tilde{q}}^\dagger)_{i,2}m_{\chi_k^0}\Big[e_q e\mathcal{N}^{\gamma}_{\tilde{g}(2)}\mathcal{Q}_2+g_3\mathcal{N}^{g(a)}_{\chi_k^0(2)}\mathcal{Q}_4\Big]\Big\} \\
& +\frac{2}{3}\frac{e^2 g_3^2}{s_{\rm w}^2 c_{\rm w}^2}\int\frac{d^Dq_1}{(2\pi)^D}\frac{d^Dq_2}{(2\pi)^D}\frac{1}{\mathcal{D}^{(b)}_{\chi_k^0}} \\
& \times\Big\{-(\mathcal{Z}_{\tilde{q}})_{2,j}(B_N^q)^\dagger_{jk}(\mathcal{Z}_{\tilde{q}})_{1,i}(B_N^q)^\dagger_{ik}m_{\chi_k^0}\Big[e_q e\mathcal{N}^{\gamma(b)}_{\chi_k^0(1)}\mathcal{Q}_1+g_3\mathcal{N}^{g(b)}_{\chi_k^0(1)}\mathcal{Q}_3\Big] \\
& -(\mathcal{Z}_{\tilde{q}})_{1,j}(A_N^q)^\dagger_{jk}(\mathcal{Z}_{\tilde{q}})_{2,i}(A_N^q)^\dagger_{ik}m_{\chi_k^0}\Big[e_q e\mathcal{N}^{\gamma(b)}_{\chi_k^0(1)}\mathcal{Q}_2+g_3\mathcal{N}^{g(b)}_{\chi_k^0(1)}\mathcal{Q}_4\Big] \\
& +(\mathcal{Z}_{\tilde{q}})_{2,j}(A_N^q)^\dagger_{jk}(\mathcal{Z}_{\tilde{q}})_{2,i}(B_N^q)^\dagger_{ik}|m_{\tilde{g}}|e^{-i\theta_3}\Big[e_q e\mathcal{N}^{\gamma(b)}_{\chi_k^0(2)}\mathcal{Q}_1+g_3\mathcal{N}^{g(b)}_{\chi_k^0(2)}\mathcal{Q}_3\Big] \\
& +(\mathcal{Z}_{\tilde{q}})_{1,j}(B_N^q)^\dagger_{jk}(\mathcal{Z}_{\tilde{q}})_{1,i}(A_N^q)^\dagger_{ik}|m_{\tilde{g}}|e^{i\theta_3}\Big[e_q e\mathcal{N}^{\gamma(b)}_{\chi_k^0(2)}\mathcal{Q}_2+g_3\mathcal{N}^{g(b)}_{\chi_k^0(2)}\mathcal{Q}_4\Big]\Big\}+\cdots \qquad (16)
\end{aligned}
$$

with $\mathcal{D}^{(a)}_{\chi_k^0}=((q_2-q_1)^2-m_q^2)(q_1^2-m^2_{\chi_k^0})(q_1^2-m^2_{\tilde{q}_j})(q_2^2-m^2_{\tilde{q}_i})(q_2^2-|m_{\tilde{g}}|^2)$, $\mathcal{D}^{(b)}_{\chi_k^0}=\mathcal{D}^{(a)}_{\chi_k^0}(m^2_{\chi_k^0}\leftrightarrow|m_{\tilde{g}}|^2)$. The form factors $\mathcal{N}^{\gamma(b)}_{\chi_k^0(1,2)}=\mathcal{N}^{\gamma}_{\tilde{g}(1,2)}(|m_{\tilde{g}}|^2\to m^2_{\chi_k^0})$. The explicit expressions of the form factors $\mathcal{N}^{g(a,b)}_{\chi_k^0(1,2)}$ are presented in appendix A.

With a help of Eq. (11), one finds the following identities:

$$
\begin{aligned}
& \int\frac{d^Dq_1}{(2\pi)^D}\frac{d^Dq_2}{(2\pi)^D}\frac{\mathcal{N}^{\gamma(b)}_{\chi_k^0(1)},\mathcal{N}^{g(b)}_{\chi_k^0(1)}}{\mathcal{D}^{(b)}_{\chi_k^0}}\Big(\tilde{q}_i\leftrightarrow\tilde{q}_j,\ q_1\leftrightarrow q_2\Big) \\
= & \int\frac{d^Dq_1}{(2\pi)^D}\frac{d^Dq_2}{(2\pi)^D}\frac{\mathcal{N}^{\gamma}_{\tilde{g}(2)},\mathcal{N}^{g(a)}_{\chi_k^0(2)}}{\mathcal{D}^{(a)}_{\chi_k^0}}\,, \\
& \int\frac{d^Dq_1}{(2\pi)^D}\frac{d^Dq_2}{(2\pi)^D}\frac{\mathcal{N}^{\gamma(b)}_{\chi_k^0(1)},\mathcal{N}^{g(b)}_{\chi_k^0(1)}}{\mathcal{D}^{(b)}_{\chi_k^0}}\Big(\tilde{q}_i\leftrightarrow\tilde{q}_j,\ q_1\leftrightarrow q_2\Big) \\
= & \int\frac{d^Dq_1}{(2\pi)^D}\frac{d^Dq_2}{(2\pi)^D}\frac{\mathcal{N}^{\gamma}_{\tilde{g}(2)},\mathcal{N}^{g(a)}_{\chi_k^0(2)}}{\mathcal{D}^{(a)}_{\chi_k^0}}\,, \\
& \int\frac{d^Dq_1}{(2\pi)^D}\frac{d^Dq_2}{(2\pi)^D}\frac{\mathcal{N}^{\gamma(b)}_{\chi_k^0(2)},\mathcal{N}^{g(b)}_{\chi_k^0(2)}}{\mathcal{D}^{(b)}_{\chi_k^0}}\Big(\tilde{q}_i\leftrightarrow\tilde{q}_j,\ q_1\leftrightarrow q_2\Big)
\end{aligned}
$$

$$
\begin{aligned}
&= \int \frac{d^Dq_1}{(2\pi)^D}\frac{d^Dq_2}{(2\pi)^D}\frac{\mathcal{N}^{\gamma}_{\tilde{g}(1)},\mathcal{N}^{g(a)}_{\chi^0_k(1)}}{\mathcal{D}^{(a)}_{\chi^0_k}}\,,\\
&\quad \int \frac{d^Dq_1}{(2\pi)^D}\frac{d^Dq_2}{(2\pi)^D}\frac{\mathcal{N}^{\gamma(b)}_{\chi^0_k(2)},\mathcal{N}^{g(b)}_{\chi^0_k(2)}}{\mathcal{D}^{(b)}_{\chi^0_k}}\Big(\tilde{q}_i\leftrightarrow\tilde{q}_j,\ q_1\leftrightarrow q_2\Big)\\
&= \int \frac{d^Dq_1}{(2\pi)^D}\frac{d^Dq_2}{(2\pi)^D}\frac{\mathcal{N}^{\gamma}_{\tilde{g}(1)},\mathcal{N}^{g(a)}_{\chi^0_k(1)}}{\mathcal{D}^{(a)}_{\chi^0_k}}\,. \qquad (17)
\end{aligned}
$$

Substituting these identities into eq.(15) and removing the ultra-violet divergence in $\overline{MS}$ scheme, we may extract the two-loop "neutralino-gluino" corrections to the quark EDMs and CEDMs:

$$
\begin{aligned}
d^{\gamma}_{\chi^0_k(2)} &= \frac{4e_q e\alpha\alpha_s}{3(4\pi)^2 s^2_{\rm w}c^2_{\rm w}m^2_{\rm w}}\Big\{|m_{\tilde{g}}|F_1(x_q,x_{\tilde{q}_j},x_{\tilde{g}},x_{\chi^0_k},x_{\tilde{q}_i})\Big[\mathbf{Im}\Big((A^q_N)_{kj}(\mathcal{Z}^{\dagger}_{\tilde{q}})_{j,1}\\
&\quad\times(B^q_N)_{ki}(\mathcal{Z}^{\dagger}_{\tilde{q}})_{i,1}e^{-i\theta_3}\Big)-\mathbf{Im}\Big((B^q_N)_{kj}(\mathcal{Z}^{\dagger}_{\tilde{q}})_{j,2}(A^q_N)_{ki}(\mathcal{Z}^{\dagger}_{\tilde{q}})_{i,2}e^{i\theta_3}\Big)\Big]\\
&\quad -m_{\chi^0_k}F_2(x_q,x_{\tilde{q}_j},x_{\tilde{g}},x_{\chi^0_k},x_{\tilde{q}_i})\Big[\mathbf{Im}\Big((A^q_N)_{kj}(\mathcal{Z}^{\dagger}_{\tilde{q}})_{j,2}(A^q_N)_{ki}(\mathcal{Z}^{\dagger}_{\tilde{q}})_{i,1}\Big)\\
&\quad -\mathbf{Im}\Big((B^q_N)_{kj}(\mathcal{Z}^{\dagger}_{\tilde{q}})_{j,1}(B^q_N)_{ki}(\mathcal{Z}^{\dagger}_{\tilde{q}})_{i,2}\Big)\Big]\Big\}\,,\\
d^{g}_{\chi^0_k(2)} &= \frac{4g_3\alpha\alpha_s}{3(4\pi)^2 s^2_{\rm w}c^2_{\rm w}m^2_{\rm w}}\Big\{|m_{\tilde{g}}|F_4(x_q,x_{\tilde{q}_j},x_{\tilde{g}},x_{\chi^0_k},x_{\tilde{q}_i})\Big[\mathbf{Im}\Big((A^q_N)_{kj}(\mathcal{Z}^{\dagger}_{\tilde{q}})_{j,1}\\
&\quad\times(B^q_N)_{ki}(\mathcal{Z}^{\dagger}_{\tilde{q}})_{i,1}e^{-i\theta_3}\Big)-\mathbf{Im}\Big((B^q_N)_{kj}(\mathcal{Z}^{\dagger}_{\tilde{q}})_{j,2}(A^q_N)_{ki}(\mathcal{Z}^{\dagger}_{\tilde{q}})_{i,2}e^{i\theta_3}\Big)\Big]\\
&\quad -m_{\chi^0_k}F_5(x_q,x_{\tilde{q}_j},x_{\tilde{g}},x_{\chi^0_k},x_{\tilde{q}_i})\Big[\mathbf{Im}\Big((A^q_N)_{kj}(\mathcal{Z}^{\dagger}_{\tilde{q}})_{j,2}(A^q_N)_{ki}(\mathcal{Z}^{\dagger}_{\tilde{q}})_{i,1}\Big)\\
&\quad -\mathbf{Im}\Big((B^q_N)_{kj}(\mathcal{Z}^{\dagger}_{\tilde{q}})_{j,1}(B^q_N)_{ki}(\mathcal{Z}^{\dagger}_{\tilde{q}})_{i,2}\Big)\Big]\Big\}\,. \qquad (18)
\end{aligned}
$$

In a similar way, we get the following results for the two-loop "gluino-chargino" corrections:

$$
\begin{aligned}
d^{\gamma}_{\chi^{\pm}_k(2)} &= \frac{4e\alpha\alpha_s}{3(4\pi)^2 s^2_{\rm w}m^2_{\rm w}}V^{\dagger}_{qQ}V_{Qq}\Big\{|m_{\tilde{g}}|F_6(x_Q,x_{\tilde{Q}_j},x_{\tilde{g}},x_{\chi^{\pm}_k},x_{\tilde{q}_i})\Big[\mathbf{Im}\Big((A^Q_C)_{kj}(\mathcal{Z}^{\dagger}_{\tilde{Q}})_{j,1}\\
&\quad\times(B^q_C)_{ki}(\mathcal{Z}^{\dagger}_{\tilde{q}})_{i,1}e^{-i\theta_3}\Big)-\mathbf{Im}\Big((B^Q_C)_{kj}(\mathcal{Z}^{\dagger}_{\tilde{Q}})_{j,2}(A^q_C)_{ki}(\mathcal{Z}^{\dagger}_{\tilde{q}})_{i,2}e^{i\theta_3}\Big)\Big]\\
&\quad -m_{\chi^{\pm}_k}F_7(x_Q,x_{\tilde{Q}_j},x_{\tilde{g}},x_{\chi^{\pm}_k},x_{\tilde{q}_i})\Big[\mathbf{Im}\Big((A^Q_C)_{kj}(\mathcal{Z}^{\dagger}_{\tilde{Q}})_{j,2}(A^q_C)_{ki}(\mathcal{Z}^{\dagger}_{\tilde{q}})_{i,1}\Big)\\
&\quad -\mathbf{Im}\Big((B^Q_C)_{kj}(\mathcal{Z}^{\dagger}_{\tilde{Q}})_{j,1}(B^q_C)_{ki}(\mathcal{Z}^{\dagger}_{\tilde{q}})_{i,2}\Big)\Big]\Big\}\,,\\
d^{g}_{\chi^{\pm}_k(2)} &= \frac{4g_3\alpha\alpha_s}{3(4\pi)^2 s^2_{\rm w}m^2_{\rm w}}V^{\dagger}_{qQ}V_{Qq}\Big\{|m_{\tilde{g}}|F_4(x_Q,x_{\tilde{Q}_j},x_{\tilde{g}},x_{\chi^{\pm}_k},x_{\tilde{q}_i})\Big[\mathbf{Im}\Big((A^Q_C)_{kj}(\mathcal{Z}^{\dagger}_{\tilde{Q}})_{j,1}\\
&\quad\times(B^q_C)_{ki}(\mathcal{Z}^{\dagger}_{\tilde{q}})_{i,1}e^{-i\theta_3}\Big)-\mathbf{Im}\Big((B^Q_C)_{kj}(\mathcal{Z}^{\dagger}_{\tilde{Q}})_{j,2}(A^q_C)_{ki}(\mathcal{Z}^{\dagger}_{\tilde{q}})_{i,2}e^{i\theta_3}\Big)\Big]\\
&\quad -m_{\chi^{\pm}_k}F_5(x_Q,x_{\tilde{Q}_j},x_{\tilde{g}},x_{\chi^{\pm}_k},x_{\tilde{q}_i})\Big[\mathbf{Im}\Big((A^Q_C)_{kj}(\mathcal{Z}^{\dagger}_{\tilde{Q}})_{j,2}(A^q_C)_{ki}(\mathcal{Z}^{\dagger}_{\tilde{q}})_{i,1}\Big)
\end{aligned}
$$

$$-\mathbf{Im}\Big((B_C^Q)_{kj}(\mathcal{Z}_{\tilde{Q}}^\dagger)_{j,1}(B_C^q)_{ki}(\mathcal{Z}_{\tilde{q}}^\dagger)_{i,2}\Big)\Big]\Big\}\ . \tag{19}$$

Notice that the last terms of the $d^\gamma_{\chi_k^{\pm}(2)}$ and $d^g_{\chi_k^{\pm}(2)}$ are not proportional to the suppression factor $m_q/m_{\rm w}$. This implies that the two-loop "gluino-chargino" diagrams may be dominant two-loop corrections of the chargino to the quark EDMs and CEDMs.

The Wilson coefficient of the purely gluonic Weinberg operator originates from the two-loop "gluino-squark" diagrams and is given by [10]:

$$\begin{aligned} C_3 = &-3\alpha_s m_t\Big(\frac{g_3}{4\pi}\Big)^3\mathbf{Im}\Big((\mathcal{Z}_{\tilde{t}})_{2,2}(\mathcal{Z}_{\tilde{t}})^\dagger_{2,1}\Big) \\ &\times\frac{m^2_{\tilde{t}_1}-m^2_{\tilde{t}_2}}{|m_{\tilde{g}}|^5}H(\frac{m^2_{\tilde{t}_1}}{|m_{\tilde{g}}|^2},\frac{m^2_{\tilde{t}_2}}{|m_{\tilde{g}}|^2},\frac{m^2_t}{|m_{\tilde{g}}|^2}) \end{aligned} \tag{20}$$

where $\mathcal{Z}_{\tilde{t}}$ is the diagonalizing matrix for the squared mass matrix of stop, and the function H is the same as that given in [10].

In order to account for the resummation of logarithmic corrections, we should evolve the quark EDMs, CEDMs and the Wilson coefficients of the Weinberg operator with the renormalization group equations (RGEs) from the matching scale Λ down to the chirality breaking scale Λ_χ [11]:

$$\begin{aligned} d_q^\gamma(\Lambda_\chi) &= \eta_\gamma d_q^\gamma(\Lambda)\ , \\ d_q^g(\Lambda_\chi) &= \eta_g d_q^g(\Lambda)\ , \\ C_3(\Lambda_\chi) &= \eta_G C_3(\Lambda)\ , \end{aligned} \tag{21}$$

where $\eta_\gamma \simeq 1.53$ and $\eta_g \simeq \eta_G \simeq 3.4$. At a low scale, the quark EDM consists of a weak interaction contribution, a quark CEDMs contribution and the contribution of the Weinberg operator. We can numerically evaluate these different contributions. According to a naive dimensional analysis one can write [12]

$$d_q = d_q^\gamma + \frac{e}{4\pi}d_q^g + \frac{e\Lambda_\chi}{4\pi}C_3(\Lambda_\chi)\ . \tag{22}$$

The EDM of the neutron is, on the basis of the simple SU(6) quark model, then given by

$$d_n = \frac{1}{3}(4d_d - d_u)\ , \tag{23}$$

where d_u, d_d are the EDMs of the up- and down-type quarks respectively.

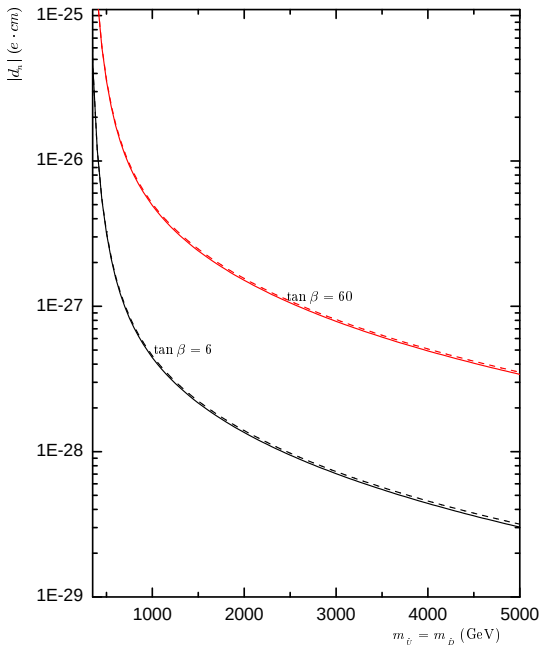

FIG. 3: The correction from one-loop gluino diagrams (Eq. 4) and that from two-loop gluino-gluino diagrams (Eq. 15) versus the right handed squark masses $m_{\tilde{U}} = m_{\tilde{D}}$ with $\theta_3 = arg(m_{\tilde{g}}) = \pi/2$, $\tan\beta = 6$ (60), and $m_{\tilde{Q}_1} = 20$ TeV, where the dash-lines represent one-loop results and the solid-lines correspond to a sum of the one- and two-loop results.

III. THE NUMERICAL ANALYSIS

The MSSM Lagrangian contains several sources for CP violating phases: the phases of the μ parameter in the superpotential and the corresponding bilinear coupling of the soft breaking terms, three phases of the gaugino mass terms, and the phases of the trilinear sfermion Yukawa couplings in the soft Lagrangian. As we are not considering the spontaneous CP violation in this work, the CP phase of soft bilinear coupling vanishes due to the tree level neutral Higgs tadpole conditions.

As we remarked above, the two-loop gluino corrections to the neutron EDM are important, and may be the dominant contribution in a certain part of the parameter space. Let us clarify this point in some detail by means of numerical analysis. Without losing too much generality, we will fix the following values for the supersymmetric parameters: $|\mu| = |m_{\lambda_B}| = |m_{\lambda_A}| = |m_{\tilde{g}}| = 300$ GeV, [1] $|A_q| = 100$ GeV ($q = u,\ d,\ c,\ s,\ t,\ b$), and

[1] m_{λ_B}, m_{λ_A} are the soft masses of $U(1) \times SU(2)$ gauginos respectively.

$m_{\tilde{Q}_2} = 20$ TeV, $m_{\tilde{Q}_3} = 5$ TeV, $m_{\tilde{C}} = m_{\tilde{S}} = 5$ TeV, $m_{\tilde{T}} = m_{\tilde{B}} = 200$ GeV in our numerical analysis. For simplification, we will also assume $\varphi_q = arg(A_q) = 0$, $\theta_\mu = arg(\mu) = 0$.

In Fig. 3 we present the corrections the neutron EDM obtains from the one-loop "gluino-squark" diagrams (see Eq. (4) and Fig. 1) and two-loop "gluino-gluino" contributions (see Eq. (15) and Fig. 2) as a function of the right-handed squark masses $m_{\tilde{U}} = m_{\tilde{D}}$. We have set in this figure $\theta_1 = arg(m_{\lambda_B}) = 0$, $\theta_2 = arg(m_{\lambda_A}) = 0$, $\theta_3 = arg(m_{\tilde{g}}) = \pi/2$, $\tan\beta = 6$ (60), and $m_{\tilde{Q}_1} = 20$ TeV, and what are plotted are the one-loop "gluino-squark" contribution (dashed line) and the sum of the one-loop "gluino-squark" and two-loop "gluino-gluino" contributions (solid line). The dependence of the contributions on the CP violation phase θ_3 are all proportional to the factor $\mathbf{Im}\Big((\mathcal{Z}_{\tilde{q}})_{2,j}(\mathcal{Z}^\dagger_{\tilde{q}})_{j,1}e^{-i\theta_3}\Big)$, and the two-loop correction is less than 10% of the one-loop results for our choice of the parameter values. The neutron EDM depends on the parameter $\tan\beta$ through the squark mixing matrices, and as seen from the plots, this makes the a large difference between the corrections in a low and a high $\tan\beta$ cases.

Let us now focus on the two-loop gluino corrections of the neutron EDM. There the CP violating phases θ_1, θ_2 induce a nonzero quark EDMs at one-loop level (see Eq. (6)) through the neutralino mixing matrix, whereas the CP phase θ_3 contributes only through the two-loop diagrams (see Eq. (18)). We will present three sets of plots, where we set one of the phases $\theta_1, \theta_2, \theta_3$ at a time equal to $\pi/2$ while the other two are set equal to zero. Taking first $\theta_1 = \pi/2$, $\theta_2 = \theta_3 = 0$ and $\tan\beta = 6$ (60), we plot in Fig. 4 for two values of $\tan\beta$ the neutron EDM as a function of the soft squark masses $m_{\tilde{Q}_1} = m_{\tilde{U}} = m_{\tilde{D}}$. In this plot the dash-lines represent the one-loop "neutralino-squark" results and the solid-lines correspond to a sum of one-loop "neutralino-squark" and two-loop "neutralino-gluino" contributions.

In Fig. 5 we present the same plot for the case $\theta_2 = \pi/2$, $\theta_1 = \theta_3 = 0$, other parameters being the same as in Fig. 4. We notice that the two-loop gluino corrections to the one-loop results can be as large as about 20%. For the contribution of neutralino to the neutron EDM, the most interesting piece originates from the CP violating phase of the gluino mass, which does not contribute at the one-loop level.

In Fig. 6 we plot the neutron EDM versus the soft squark masses $m_{\tilde{Q}_1} = m_{\tilde{U}} = m_{\tilde{D}}$ in the case $\theta_3 = \pi/2$, $\theta_1 = \theta_2 = 0$, the other parameters are taken as in Fig. 4. As the soft squark masses increase, the neutron EDM d_n varies steeply. Because of the interference between the up- and down-quark EDMs (see Eq. 23), there is in the case of $\tan\beta = 6$ a profound

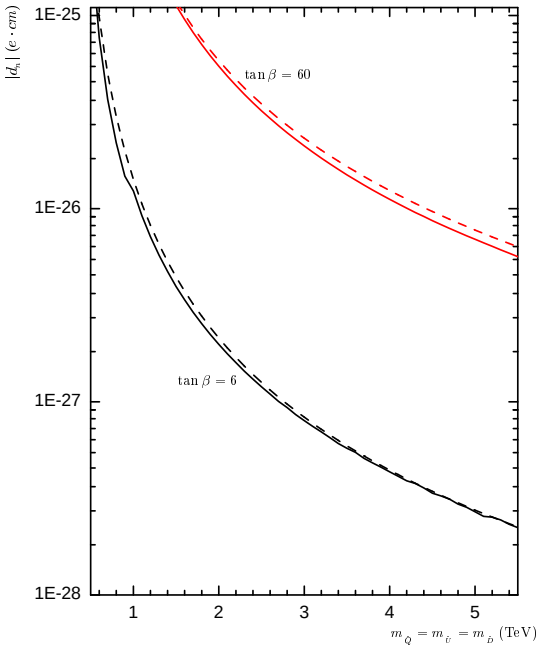

FIG. 4: The correction from one-loop neutralino diagrams (Eq. 6) and that from two-loop neutralino-gluino diagrams (Eq. 18) versus the squark masses $m_{\tilde{Q}_1} = m_{\tilde{U}} = m_{\tilde{D}}$ with $\theta_1 = \pi/2,\ \theta_2 = \theta_3 = 0,\ \tan\beta = 6$ (60), where the dash-lines represent one-loop results and the solid-lines correspond to a sum of the one- and two-loop results.

minimum at $m_{\tilde{Q}_1} = m_{\tilde{U}} = m_{\tilde{D}} \sim 900$ GeV .

Let us move to the corrections arising from the diagrams involving virtual charginos. In this case the phase θ_1 does not contribute to the quark EDMs at all, whereas θ_2 contributes at one-loop level (see Eq. (8)) and θ_3 takes part in the game through only two-loop diagrams (see Eq. (19)). At the one-loop level, the chargino contributions to the quark EDMs are proportional to the suppression factor m_q/m_z $(q = u,\ d)$. However, the last terms of the two-loop "gluino-chargino" corrections to the quark EDMs and CEDMs, given in Eq. (19), do not depend on this suppression factor. Taking $\theta_2 = \pi/2,\ \theta_3 = 0$, we plot in Fig. 7 the neutron EDM as a function of the soft squark masses $m_{\tilde{Q}_1} = m_{\tilde{U}} = m_{\tilde{D}}$ for a large $\tan\beta$. The dash lines represent the one-loop "chargino-squark" results and the solid lines correspond to the sum of the one-loop "chargino-squark" and two-loop "chargino-gluino" results. As the dominant two-loop "gluino-chargino" corrections are not proportional to the suppression factor given above, they play the leading role. The corresponding figure for a low $\tan\beta$ is presented in Fig. 8.

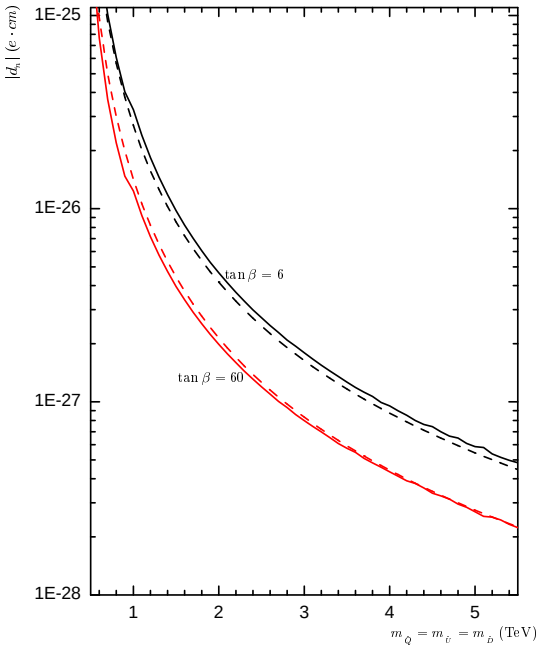

FIG. 5: The correction from one-loop neutralino diagrams (Eq. 6) only and the sum of one-loop neutralino and two-loop neutralino-gluino diagrams (Eq. 18) versus the squark masses $m_{\tilde{Q}_1} = m_{\tilde{U}} = m_{\tilde{D}}$ with $\theta_2 = \pi/2,\ \theta_1 = \theta_3 = 0,\ \tan\beta = 6\ (60)$, where the dash-lines represent one-loop results and the solid-lines correspond to a sum of the one- and two-loop results.

Just as in the neutralino case, the CP phase θ_3 affects also in the chargino case the quark EDMs only at the two-loop level. In Fig. 9 we show the variation of the neutron EDM with respect to $m_{\tilde{Q}_1} = m_{\tilde{U}} = m_{\tilde{D}}$ in the case $\theta_3 = \pi/2,\ \theta_2 = 0$ and $\tan\beta = 6\ (60)$. Even when the squark masses are larger than 1 TeV, the neutron EDM induced by the CP phase θ_3 can be close to $1.1 \times 10^{-25}\ (e \cdot cm)$, which is the present upper bound from experiments.

By including all the contributions present in Eq. (22), we now determine in our theoretical framework the variation of the neutron EDM as a function of the CP phase θ_3. Taking $\theta_1 = \theta_2 = 0,\ m_{\tilde{Q}_1} = m_{\tilde{U}} = m_{\tilde{D}} = 2.3$ TeV and $\tan\beta = 60$, we plot in Fig. 10 the neutron EDM versus the CP phase θ_3 , where the dashed line is the sum of the one-loop results and the contributions of the Weinberg operator, and the solid line represents the results including two-loop gluino corrections to the quark dipole moment operators. Fig. 11 gives the corresponding plot for the case $\tan\beta = 6$. It is clear that the two-loop gluino corrections can reach the 30% level for our choice of the parameters.

In this work, we do not consider the effects of the CP phases associated with the trilinear

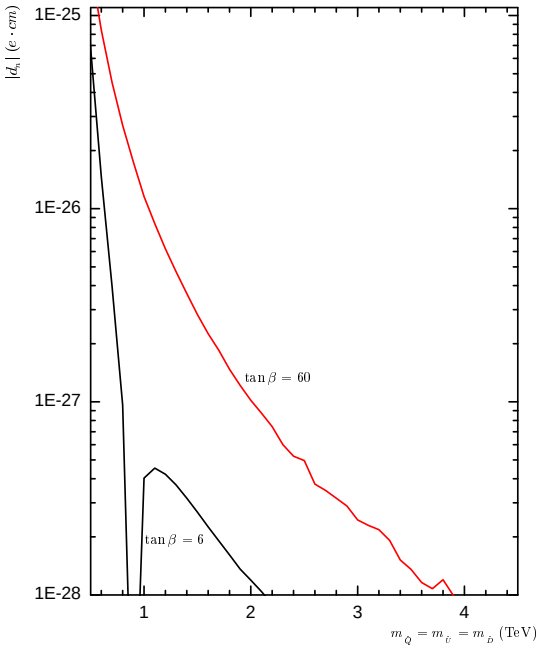

FIG. 6: The correction the two-loop neutralino-gluino diagrams (Eq. 18) versus the squark masses $m_{\tilde{Q}_1} = m_{\tilde{U}} = m_{\tilde{D}}$ with $\theta_3 = \pi/2,\ \theta_1 = \theta_2 = 0,\ \tan\beta = 6\ (60)$. With the choice on parameter space, the one-loop neutralino contribution to neutron EDM is zero.

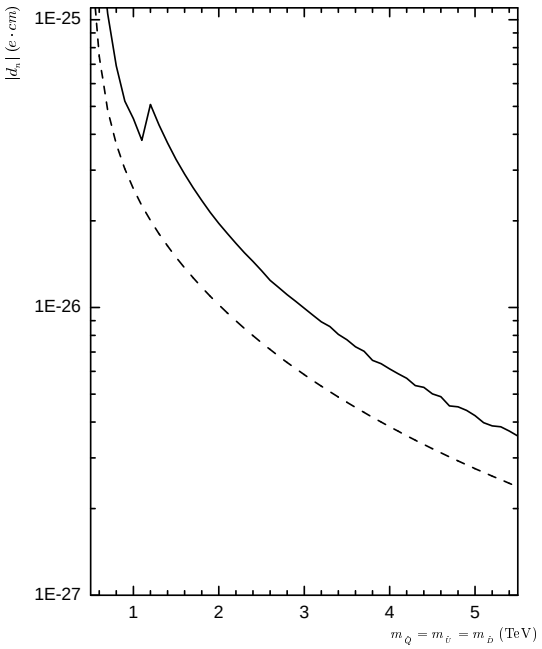

FIG. 7: The correction from one-loop chargino diagrams (Eq. 8) and the sum of one- and two-loop chargino-gluino diagrams (Eq. 19) versus the squark masses $m_{\tilde{Q}_1} = m_{\tilde{U}} = m_{\tilde{D}}$ with $\theta_2 = \pi/2,\ \theta_3 = 0,\ \tan\beta = 60$.

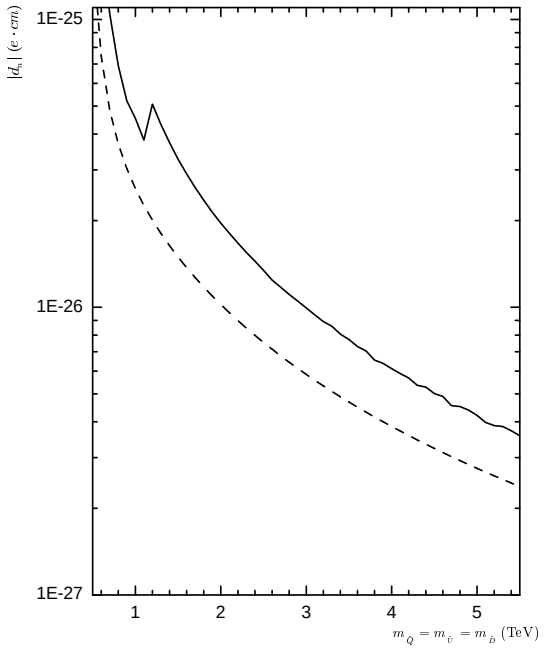

FIG. 8: The correction from one-loop chargino diagrams (Eq. 8) and the sum of one- and two-loop chargino-gluino diagrams (Eq. 19) versus the squark masses $m_{\tilde{Q}_1} = m_{\tilde{U}} = m_{\tilde{D}}$ with $\theta_2 = \pi/2,\ \theta_3 = 0,\ \tan\beta = 6$.

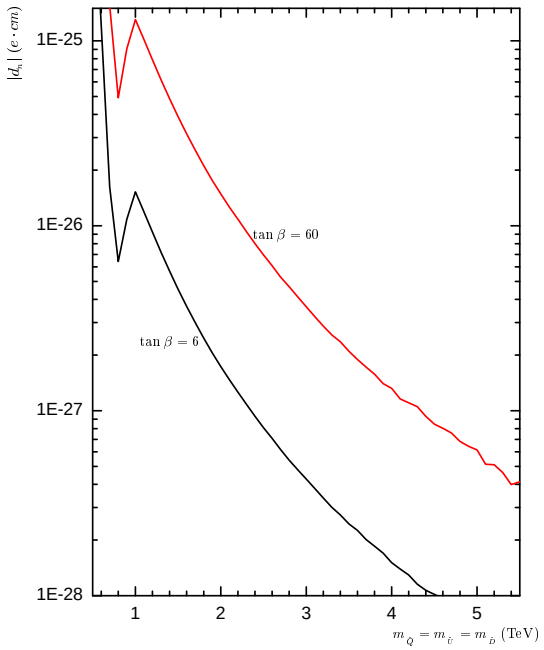

FIG. 9: The correction from the two-loop chargino-gluino diagrams (Eq. 19) versus the squark masses $m_{\tilde{Q}_1} = m_{\tilde{U}} = m_{\tilde{D}}$ with $\theta_3 = \pi/2,\ \theta_1 = \theta_2 = 0,\ \tan\beta = 6,$ (60).

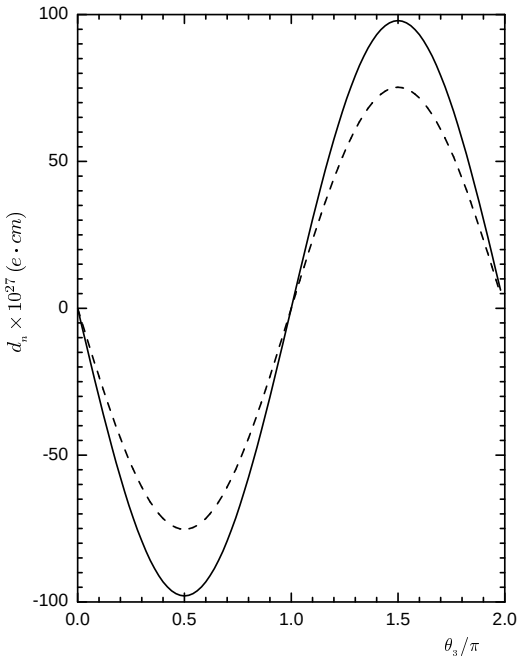

FIG. 10: Taking $\theta_1 = \theta_2 = 0$, $m_{\tilde{Q}_1} = m_{\tilde{U}} = m_{\tilde{D}} = 2.3$ TeV and $\tan\beta = 60$, the neutron EDM varies with the CP phase θ_3.

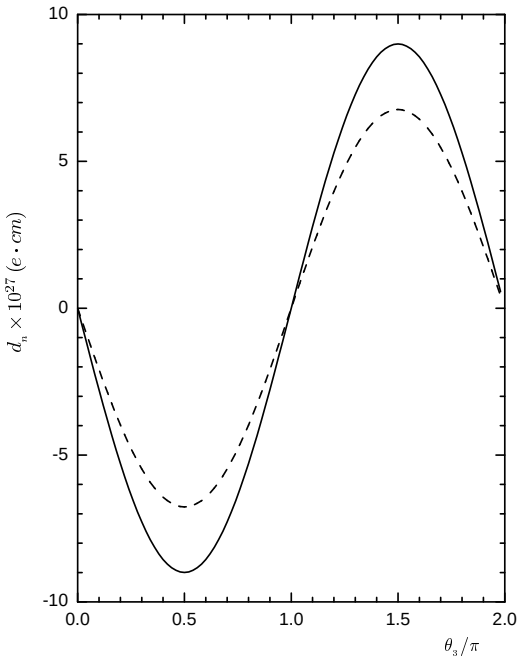

FIG. 11: Taking $\theta_1 = \theta_2 = 0$, $m_{\tilde{Q}_1} = m_{\tilde{U}} = m_{\tilde{D}} = 2.3$ TeV and $\tan\beta = 6$, the neutron EDM varies with the CP phase θ_3.

soft squark Yukawa coupling. This is reflected in our numerical results as a relatively strong decrease of the neutron EDM as a function increasing squark masses. Moreover, for the model we employ here, the mass of the lightest Higgs boson sets a strong constraint on the parameter space of the new physics. As indicated in the literature [13], the CP violation would cause changes to the neutral-Higgs-quark coupling, neutral Higgs-gauge-boson coupling and self-coupling of Higgs boson. The present experimental lower bound for the mass of the lightest Higgs boson is relaxed to 60 GeV. In our numerical analysis we have taken this constraint for the parameter space into account.

IV. THE CONCLUSION

We have investigated in this work the corrections induced by some two-loop gluino diagrams to the neutron EDM. Except a loop factor, the two-loop contributions do not involve other suppression factors. Since the dependence of the two-loop corrections on the relevant CP violating phases differs from that of the one-loop corrections, there is a region in the parameter space, where the two-loop corrections are comparable with the one-loop corrections. Certainly, the present experimental upper bound on the neutron EDM would set a very rigorous constraint on the possible values of CP phases if the masses of new particles are in the TeV range. In order to circumvent this constraint, one can assume, as was done in the corresponding analysis at one-loop level, that the squarks of the first two generations are heavy, *i.e.* ≥ 2 TeV, or invoke a mechanism that causes an effective cancellation among different contributions to the quark EDMs.

Because the exact analytical expressions for the two-loop vacuum integrals are derivable, one can extract, at least in principle, the Wilson coefficients of the dipole moment operators from any two-loop triangle diagrams and thereby find their contributions to the fermion anomalous magnetic dipole moments and EDMs. We will address our analysis to this issue in our coming works.

Acknowledgments

The work has been supported by the Academy of Finland under the contracts no. 104915 and 107293, and partly also by the National Natural Sceince Foundation of China.

APPENDIX A: THE FORM FACTORS

$$
\begin{aligned}
\mathcal{N}^{\gamma}_{\tilde{g}(1)} =& -\frac{4}{D}\frac{q_1^2 q_1\cdot(q_2-q_1)}{(q_1^2-m^2_{\tilde{q}_j})^2}+\frac{q_1\cdot(q_2-q_1)}{q_1^2-m^2_{\tilde{q}_j}}-\frac{4}{D}\frac{q_1\cdot(q_2-q_1)q_2^2}{(q_2^2-|m_{\tilde{g}}|^2)^2}\\
&+\frac{q_1\cdot(q_2-q_1)}{q_2^2-|m_{\tilde{g}}|^2}+\frac{4}{(q_1^2-m^2_{\tilde{q}_j})(q_2^2-|m_{\tilde{g}}|^2)}\Big[\frac{q_1^2 q_1\cdot q_2}{D}\\
&-\frac{D(q_1\cdot q_2)^2-q_1^2q_2^2}{D(D-1)}\Big]+\frac{D-2}{D}\frac{q_1\cdot(q_2-q_1)}{(q_2-q_1)^2-m_q^2}\ ,\\
\mathcal{N}^{\gamma}_{\tilde{g}(2)} =& \frac{2}{D}\frac{q_2\cdot(q_2-q_1)}{q_2^2-m^2_{\tilde{q}_i}}+\frac{4}{D}\frac{q_1^2 q_2\cdot(q_2-q_1)}{(q_1^2-m^2_{\tilde{q}_j})^2}-\frac{q_2\cdot(q_2-q_1)}{q_1^2-m^2_{\tilde{q}_j}}\\
&+\frac{4}{(q_1^2-m^2_{\tilde{q}_j})(q_2^2-|m_{\tilde{g}}|^2)}\Big[\frac{q_1\cdot q_2 q_2^2}{D}-\frac{D(q_1\cdot q_2)^2-q_1^2q_2^2}{D(D-1)}\Big]\\
&+\frac{4}{D}\frac{q_2^2 q_2\cdot(q_2-q_1)}{(q_2^2-|m_{\tilde{g}}|^2)^2}-\frac{2+D}{D}\frac{q_2\cdot(q_2-q_1)}{q_2^2-|m_{\tilde{g}}|^2}+\frac{2-D}{D}\frac{q_2\cdot(q_2-q_1)}{(q_2-q_1)^2-m_q^2}\ ,\\
\mathcal{N}^{g}_{\tilde{g}(1)} =& -\frac{4}{D}\frac{q_1^2 q_1\cdot(q_2-q_1)}{(q_1^2-m^2_{\tilde{q}_j})^2}+\frac{17}{8}\frac{q_1\cdot(q_2-q_1)}{q_1^2-m^2_{\tilde{q}_j}}-\frac{4}{D}\frac{q_1\cdot(q_2-q_1)q_2^2}{(q_2^2-|m_{\tilde{g}}|^2)^2}\\
&+\frac{4}{(q_1^2-m^2_{\tilde{q}_j})(q_2^2-|m_{\tilde{g}}|^2)}\Big[\frac{q_1^2 q_1\cdot q_2}{D}-\frac{D(q_1\cdot q_2)^2-q_1^2q_2^2}{D(D-1)}\Big]\\
&-\frac{1}{8}\frac{q_1\cdot(q_2-q_1)}{q_2^2-|m_{\tilde{g}}|^2}-\frac{18-9D}{8D}\Big[\frac{q_2\cdot(q_2-q_1)}{q_2^2-|m_{\tilde{g}}|^2}+\frac{q_2\cdot(q_2-q_1)}{q_2^2-m^2_{\tilde{q}_i}}\Big]\\
&+\frac{10}{8}\frac{2-D}{D}\frac{q_1\cdot(q_2-q_1)}{(q_2-q_1)^2-m_q^2}\ ,\\
\mathcal{N}^{g}_{\tilde{g}(2)} =& \frac{4}{D}\frac{q_1^2 q_2\cdot(q_2-q_1)}{(q_1^2-m^2_{\tilde{q}_j})^2}+\frac{4}{D}\frac{q_2^2 q_2\cdot(q_2-q_1)}{(q_2^2-|m_{\tilde{g}}|^2)^2}-\frac{q_2\cdot(q_2-q_1)}{q_1^2-m^2_{\tilde{q}_j}}\\
&-\frac{34-D}{8D}\frac{q_2\cdot(q_2-q_1)}{q_2^2-|m_{\tilde{g}}|^2}+\frac{4}{(q_1^2-m^2_{\tilde{q}_j})(q_2^2-|m_{\tilde{g}}|^2)}\Big[\frac{q_1\cdot q_2 q_2^2}{D}\\
&-\frac{D(q_1\cdot q_2)^2-q_1^2q_2^2}{D(D-1)}\Big]-\frac{1}{4D}\frac{q_2\cdot(q_2-q_1)}{q_2^2-m^2_{\tilde{q}_i}}+\frac{9}{8}\frac{q_2\cdot(q_2-q_1)}{q_1^2-|m_{\tilde{g}}|^2}\\
&-\frac{10}{8}\frac{2-D}{D}\frac{q_2\cdot(q_2-q_1)}{(q_2-q_1)^2-m_q^2}\ ,\\
\mathcal{N}^{g(a)}_{\chi^0_k(1)} =& -\frac{4}{D}\frac{q_1^2 q_1\cdot(q_2-q_1)}{(q_1^2-m^2_{\tilde{q}_j})^2}+\frac{q_1\cdot(q_2-q_1)}{q_1^2-m^2_{\tilde{q}_j}}-\frac{4}{D}\frac{q_1\cdot(q_2-q_1)q_2^2}{(q_2^2-|m_{\tilde{g}}|^2)^2}\\
&-\frac{1}{8}\frac{q_1\cdot(q_2-q_1)}{q_2^2-|m_{\tilde{g}}|^2}+\frac{4}{(q_1^2-m^2_{\tilde{q}_j})(q_2^2-|m_{\tilde{g}}|^2)}\Big[\frac{q_1^2 q_1\cdot q_2}{D}\\
&-\frac{D(q_1\cdot q_2)^2-q_1^2q_2^2}{D(D-1)}\Big]+\frac{1}{8}\frac{2-D}{D}\frac{q_1\cdot(q_2-q_1)}{(q_2-q_1)^2-m_q^2}\ ,
\end{aligned}
$$

$$
\begin{aligned}
\mathcal{N}^{g(a)}_{\chi^0_k\,(2)} &= \frac{4}{D}\frac{q_1^2 q_2\cdot(q_2-q_1)}{(q_1^2-m^2_{\tilde{q}_j})^2}+\frac{4}{D}\frac{q_2^2 q_2\cdot(q_2-q_1)}{(q_2^2-|m_{\tilde{g}}|^2)^2}-\frac{q_2\cdot(q_2-q_1)}{q_1^2-m^2_{\tilde{q}_j}}\\
&\quad-\frac{34-D}{8D}\frac{q_2\cdot(q_2-q_1)}{q_2^2-|m_{\tilde{g}}|^2}+\frac{4}{(q_1^2-m^2_{\tilde{q}_j})(q_2^2-|m_{\tilde{g}}|^2)}\Big[\frac{q_1\cdot q_2 q_2^2}{D}\\
&\quad-\frac{D(q_1\cdot q_2)^2-q_1^2q_2^2}{D(D-1)}\Big]-\frac{1}{4D}\frac{q_2\cdot(q_2-q_1)}{q_2^2-m^2_{\tilde{q}_i}}-\frac{1}{8}\frac{2-D}{D}\frac{q_2\cdot(q_2-q_1)}{(q_2-q_1)^2-m_q^2}\,,\\
\mathcal{N}^{g(b)}_{\chi^0_k\,(1)} &= -\frac{4}{D}\frac{q_1^2 q_1\cdot(q_2-q_1)}{(q_1^2-m^2_{\tilde{q}_j})^2}+\frac{17}{8}\frac{q_1\cdot(q_2-q_1)}{q_1^2-m^2_{\tilde{q}_j}}-\frac{4}{D}\frac{q_1\cdot(q_2-q_1)q_2^2}{(q_2^2-m^2_{\chi^0_k})^2}\\
&\quad+\frac{q_1\cdot(q_2-q_1)}{q_2^2-m^2_{\chi^0_k}}+\frac{4}{(q_1^2-m^2_{\tilde{q}_j})(q_2^2-m^2_{\chi^0_k})}\Big[\frac{q_1^2 q_1\cdot q_2}{D}\\
&\quad-\frac{D(q_1\cdot q_2)^2-q_1^2q_2^2}{D(D-1)}\Big]+\frac{1}{8}\frac{2-D}{D}\frac{q_1\cdot(q_2-q_1)}{(q_2-q_1)^2-m_q^2}\\
&\quad-\frac{18-9D}{8D}\Big[\frac{q_2\cdot(q_2-q_1)}{q_2^2-m^2_{\chi^0_k}}+\frac{q_2\cdot(q_2-q_1)}{q_2^2-m^2_{\tilde{q}_i}}\Big]\,,\\
\mathcal{N}^{g(b)}_{\chi^0_k\,(2)} &= \frac{4}{D}\frac{q_1^2 q_2\cdot(q_2-q_1)}{(q_1^2-m^2_{\tilde{q}_j})^2}+\frac{4}{D}\frac{q_2^2 q_2\cdot(q_2-q_1)}{(q_2^2-m^2_{\chi^0_k})^2}-\frac{q_2\cdot(q_2-q_1)}{q_1^2-m^2_{\tilde{q}_j}}\\
&\quad-\frac{2+D}{D}\frac{q_2\cdot(q_2-q_1)}{q_2^2-m^2_{\chi^0_k}}+\frac{4}{(q_1^2-m^2_{\tilde{q}_j})(q_2^2-m^2_{\chi^0_k})}\Big[\frac{q_1\cdot q_2 q_2^2}{D}\\
&\quad-\frac{D(q_1\cdot q_2)^2-q_1^2q_2^2}{D(D-1)}\Big]+\frac{2}{D}\frac{q_2\cdot(q_2-q_1)}{q_2^2-m^2_{\tilde{q}_i}}+\frac{9}{8}\frac{q_2\cdot(q_2-q_1)}{q_1^2-|m_{\tilde{g}}|^2}\\
&\quad-\frac{1}{8}\frac{2-D}{D}\frac{q_2\cdot(q_2-q_1)}{(q_2-q_1)^2-m_q^2}\,.
\end{aligned}
\tag{A1}
$$

APPENDIX B: THE EXPRESSION OF $F_i(x_0,x_1,x_2,x_3,x_4)$ $(i=1,\ 2,\ \cdots,\ 7)$

$$
\begin{aligned}
F_1(x_0,x_1,x_2,x_3,x_4) &= \Big\{\Xi_{_A}+\Xi_{_B}+\Xi_{_C}+\Xi_{_D}+\Xi_{_E}+\frac{1}{2}\Xi_{_F}\Big\}(x_0,x_1,x_2,x_3,x_4)\,,\\
F_2(x_0,x_1,x_2,x_3,x_4) &= \Big\{\Xi_{_A}+\frac{3}{2}\Xi_{_B}+\Xi_{_C}+\Xi_{_D}+\Xi_{_E}+\frac{1}{2}\Xi_{_F}\Big\}(x_0,x_2,x_1,x_4,x_3)\\
&\quad-\frac{1}{2}\Xi_{_B}(x_0,x_4,x_1,x_2,x_3)\,,\\
F_3(x_0,x_1,x_2,x_3,x_4) &= \Big\{\Xi_{_A}+\frac{17}{8}\Xi_{_B}+\Xi_{_C}-\frac{1}{8}\Xi_{_D}+\Xi_{_E}-\frac{5}{8}\Xi_{_F}\Big\}(x_0,x_1,x_2,x_3,x_4)\\
&\quad-\frac{9}{16}\Big[\Xi_{_B}(x_0,x_2,x_1,x_4,x_3)+\Xi_{_B}(x_0,x_4,x_1,x_2,x_3)\Big]\,,\\
F_4(x_0,x_1,x_2,x_3,x_4) &= \Big\{\Xi_{_A}+\Xi_{_B}+\Xi_{_C}-\frac{1}{8}\Xi_{_D}+\Xi_{_E}-\frac{1}{16}\Xi_{_F}\Big\}(x_0,x_1,x_2,x_3,x_4)\,,
\end{aligned}
$$

$$
\begin{aligned}
F_5(x_0,x_1,x_2,x_3,x_4) &= \Big\{\Xi_{_A}+\frac{15}{16}\Xi_{_B}+\Xi_{_C}+\Xi_{_D}+\Xi_{_E}-\frac{1}{16}\Xi_{_F}\Big\}(x_0,x_2,x_1,x_4,x_3)\\
&\quad+\frac{1}{16}\Xi_{_B}(x_0,x_4,x_1,x_2,x_3)\ ,\\
F_6(x_0,x_1,x_2,x_3,x_4) &= \Big\{e_{_q}\Big[\Xi_{_A}+\Xi_{_C}+\Xi_{_D}+\Xi_{_E}\Big]+(2e_{_q}-e_{_Q})\Xi_{_B}\\
&\quad+\frac{e_{_Q}}{2}\Xi_{_F}\Big\}(x_0,x_1,x_2,x_3,x_4)-\frac{e_{_q}-e_{_Q}}{2}\Big[\Xi_{_B}(x_0,x_2,x_1,x_4,x_3)\\
&\quad+\Xi_{_B}(x_0,x_4,x_1,x_2,x_3)\Big]\ ,\\
F_7(x_0,x_1,x_2,x_3,x_4) &= \Big\{e_{_q}\Big[\Xi_{_A}+\frac{3}{2}\Xi_{_B}+\Xi_{_C}+\Xi_{_D}+\Xi_{_E}\Big]+\frac{e_{_Q}}{2}\Xi_{_F}\Big\}(x_0,x_2,x_1,x_4,x_3)\\
&\quad-\frac{e_{_q}}{2}\Xi_{_B}(x_0,x_4,x_1,x_2,x_3)-(e_{_q}-e_{_Q})\Xi_{_D}(x_0,x_2,x_3,x_4,x_1)\ .
\end{aligned}
\tag{B1}
$$

Where the functions $\Xi_{_\alpha}(x_0,x_1,x_2,x_3,x_4)$ ($\alpha=A,\ B,\ C,\ D,\ E,\ F$) are formulated as

$$
\begin{aligned}
\Xi_{_A}(x_0,x_1,x_2,x_3,x_4) &= -\frac{1}{4}\Big\{\Big[A_1-A_0-\frac{1}{2}+\frac{x_2\ln x_2-x_4\ln x_4}{x_2-x_4}\Big]\\
&\quad\times\Big[\frac{3+2\ln x_1}{x_1-x_3}-\frac{2x_1(1+2\ln x_1)}{(x_1-x_3)^2}+\frac{2(x_1^2\ln x_1-x_3^2\ln x_3)}{(x_1-x_3)^2}\Big]\\
&\quad+\frac{x_3(x_0-x_2+x_3)}{(x_1-x_3)^3(x_2-x_4)}\Phi(x_0,x_1,x_2)-\frac{x_3(x_0+x_3-x_4)}{(x_1-x_3)^3(x_2-x_4)}\Phi(x_0,x_1,x_4)\\
&\quad+\frac{x_1^2-x_0x_3-2x_1x_3+x_2x_3}{(x_1-x_3)^2(x_2-x_4)}\frac{\partial\Phi}{\partial x_1}(x_0,x_1,x_2)\\
&\quad-\frac{x_1^2-x_0x_3-2x_1x_3+x_3x_4}{(x_1-x_3)^2(x_2-x_4)}\frac{\partial\Phi}{\partial x_1}(x_0,x_1,x_4)\\
&\quad+\frac{x_1(x_0+x_1-x_2)}{2(x_1-x_3)(x_2-x_4)}\frac{\partial^2\Phi}{\partial^2 x_1}(x_0,x_1,x_2)\\
&\quad-\frac{x_1(x_0+x_1-x_4)}{2(x_1-x_3)(x_2-x_4)}\frac{\partial^2\Phi}{\partial^2 x_1}(x_0,x_1,x_4)\\
&\quad-\frac{x_3(x_0-x_2+x_3)}{(x_1-x_3)^3(x_2-x_4)}\Phi(x_0,x_3,x_2)\\
&\quad+\frac{x_3(x_0+x_3-x_4)}{(x_1-x_3)^3(x_2-x_4)}\Phi(x_0,x_3,x_4)\Big\}\ ,
\end{aligned}
\tag{B2}
$$

$$
\begin{aligned}
\Xi_{_B}(x_0,x_1,x_2,x_3,x_4) &= \frac{1}{2}\Big\{\Big[A_1-A_0+\frac{x_2\ln x_2-x_4\ln x_4}{x_2-x_4}\Big]\cdot\Big[\frac{1+\ln x_1}{x_1-x_3}\\
&\quad-\frac{x_1\ln x_1-x_3\ln x_3}{(x_1-x_3)^2}\Big]-\Big[\frac{2\ln x_1+\ln^2 x_1}{2(x_1-x_3)}-\frac{x_1\ln^2 x_1-x_3\ln^2 x_3}{2(x_1-x_3)^2}\Big]\\
&\quad-\frac{x_0-x_2+x_3}{2(x_1-x_3)^2(x_2-x_4)}\Phi(x_0,x_1,x_2)+\frac{x_0+x_1-x_2}{2(x_1-x_3)(x_2-x_4)}\frac{\partial\Phi}{\partial x_1}(x_0,x_1,x_2)\\
&\quad+\frac{x_0+x_3-x_4}{2(x_1-x_3)^2(x_2-x_4)}\Phi(x_0,x_1,x_4)-\frac{x_0+x_1-x_4}{2(x_1-x_3)(x_2-x_4)}\frac{\partial\Phi}{\partial x_1}(x_0,x_1,x_4)
\end{aligned}
$$

$$+\frac{x_0-x_2+x_3}{2(x_1-x_3)^2(x_2-x_4)}\Phi(x_0,x_3,x_2)-\frac{x_0+x_3-x_4}{2(x_1-x_3)^2(x_2-x_4)}\Phi(x_0,x_3,x_4)\Big\}\,, \quad \text{(B3)}$$

$$\begin{aligned}\Xi_{_C}(x_0,x_1,x_2,x_3,x_4)=\frac{1}{4}\Big\{&\Big[A_0+A_1+2\gamma_{_E}-2\ln(4\pi)+\frac{1}{2}-\frac{x_1\ln x_1-x_3\ln x_3}{x_1-x_3}\Big]\\
&\times\Big[\frac{3+2\ln x_2}{x_2-x_4}-\frac{2x_2(1+2\ln x_2)}{(x_2-x_4)^2}+\frac{2(x_2^2\ln x_2-x_4^2\ln x_4)}{(x_2-x_4)^3}\Big]\\
&-\frac{x_4(x_0+x_1-x_4)}{(x_1-x_3)(x_2-x_4)^3}\Phi(x_0,x_1,x_2)+\frac{x_0x_4+x_2^2-2x_2x_4+x_1x_4}{(x_1-x_3)(x_2-x_4)^2}\frac{\partial\Phi}{\partial x_2}(x_0,x_1,x_2)\\
&-\frac{x_2(x_0+x_1-x_2)}{2(x_1-x_3)(x_2-x_4)}\frac{\partial^2\Phi}{\partial^2x_2}(x_0,x_1,x_2)+\frac{x_4(x_0+x_3-x_4)}{(x_1-x_3)(x_2-x_4)^3}\Phi(x_0,x_3,x_2)\\
&-\frac{x_0x_4+x_2^2-2x_2x_4+x_3x_4}{(x_1-x_3)(x_2-x_4)^2}\frac{\partial\Phi}{\partial x_2}(x_0,x_3,x_2)+\frac{x_2(x_0-x_2+x_3)}{2(x_1-x_3)(x_2-x_4)}\frac{\partial^2\Phi}{\partial^2x_2}(x_0,x_3,x_2)\\
&+\frac{x_4(x_0+x_1-x_4)}{(x_1-x_3)(x_2-x_4)^3}\Phi(x_0,x_1,x_4)-\frac{x_4(x_0+x_3-x_4)}{(x_1-x_3)(x_2-x_4)^3}\Phi(x_0,x_3,x_4)\Big\}\,, \quad \text{(B4)}\end{aligned}$$

$$\begin{aligned}\Xi_{_D}(x_0,x_1,x_2,x_3,x_4)=\frac{1}{2}\Big\{&\Big[-2\gamma_{_E}-2\ln(4\pi)-A_0-A_1+\frac{x_1\ln x_1-x_3\ln x_3}{x_1-x_3}\Big]\\
&\times\Big[\frac{1+\ln x_2}{x_2-x_4}-\frac{x_2\ln x_2-x_4\ln x_4}{(x_2-x_4)^2}\Big]+\Big[\frac{\ln^2x_2+2\ln x_2}{2(x_2-x_4)}-\frac{x_2\ln^2x_2-x_4\ln^2x_4}{2(x_2-x_4)^2}\Big]\\
&-\frac{x_0+x_1-x_4}{2(x_1-x_3)(x_2-x_4)^2}\Phi(x_0,x_1,x_2)+\frac{x_0+x_1-x_2}{2(x_1-x_3)(x_2-x_4)}\frac{\partial\Phi}{\partial x_2}(x_0,x_1,x_2)\\
&+\frac{x_0+x_1-x_4}{2(x_1-x_3)(x_2-x_4)^2}\Phi(x_0,x_1,x_4)+\frac{x_0+x_3-x_4}{2(x_1-x_3)(x_2-x_4)^2}\Phi(x_0,x_3,x_2)\\
&-\frac{x_0-x_2+x_3}{2(x_1-x_3)(x_2-x_4)}\frac{\partial\Phi}{\partial x_2}(x_0,x_3,x_2)-\frac{x_0+x_3-x_4}{2(x_1-x_3)(x_2-x_4)^2}\Phi(x_0,x_3,x_4)\Big\}\,, \quad \text{(B5)}\end{aligned}$$

$$\begin{aligned}\Xi_{_E}(x_0,x_1,x_2,x_3,x_4)=\frac{1}{6}\Big\{&(A_1-A_0)\cdot\Big[\frac{1+\ln x_2}{x_2-x_4}-\frac{x_2\ln x_2-x_4\ln x_4}{(x_2-x_4)^2}-\frac{2+2\ln x_1}{x_1-x_3}\\
&+\frac{2(x_1\ln x_1-x_3\ln x_3)}{(x_1-x_3)^2}\Big]+3\Big[\frac{x_1+2x_1\ln x_1}{x_1-x_3}-\frac{x_1^2\ln x_1-x_3^2\ln x_3}{(x_1-x_3)^2}\Big]\cdot\Big[\frac{1+\ln x_2}{x_2-x_4}\\
&-\frac{x_2\ln x_2-x_4\ln x_4}{(x_2-x_4)^2}\Big]-\frac{3}{2}\Big[\frac{x_2+2x_2\ln x_2}{x_2-x_4}-\frac{x_2^2\ln x_2-x_4^2\ln x_4}{(x_2-x_4)^2}\Big]+\frac{\ln x_1+2\ln x_1}{x_1-x_3}\\
&-\frac{(x_1\ln^2x_1-x_3\ln^2x_3)}{(x_1-x_3)^2}+\frac{\ln x_2+2\ln x_2}{x_2-x_4}-\frac{(x_2\ln^2x_2-x_4\ln^2x_4)}{(x_2-x_4)^2}\\
&+\frac{2[x_1^2x_4+x_2^2x_3+(x_0-2x_1-2x_2)x_3x_4]}{(x_1-x_3)^2(x_2-x_4)^2}\ln x_1\ln x_2\\
&-\frac{2[x_1^2-x_2x_3-2x_1x_3+x_0x_3]}{(x_1-x_3)^2(x_2-x_4)}\ln x_1-\frac{2[x_2^2-x_1x_4-2x_2x_4+x_0x_4]}{(x_1-x_3)(x_2-x_4)^2}\ln x_2\end{aligned}$$

$$
\begin{aligned}
&-\frac{2(x_1+x_2-x_0)}{(x_1-x_3)(x_2-x_4)}-\frac{2x_4[x_1^2+x_3(x_0-2x_1-x_4)]}{(x_1-x_3)^2(x_2-x_4)^2}\ln x_1\ln x_4\\
&-\frac{2x_4(x_1+x_4-x_0)}{(x_1-x_3)(x_2-x_4)^2}\ln x_4-\frac{2x_3[x_2^2+x_4(x_0-2x_2-x_3)]}{(x_1-x_3)^2(x_2-x_4)^2}\ln x_2\ln x_3\\
&-\frac{2x_3(x_2+x_3-x_0)}{(x_1-x_3)^2(x_2-x_4)}\ln x_3-\frac{2x_3x_4(x_3+x_4-x_0)}{(x_1-x_3)^2(x_2-x_4)^2}\ln x_3\ln x_4\\
&+\frac{\Phi(x_0,x_1,x_2)}{2(x_1-x_3)^2(x_2-x_4)^2}\Big[2x_0^2+x_1^2-2x_2^2-x_0x_3-4x_0x_4-2x_1x_3+4x_2x_4+x_3x_4\Big]\\
&+\frac{x_1^2-2x_0^2+2x_2^2+x_0x_1+4x_0x_4-x_1x_4-4x_2x_4}{2(x_1-x_3)(x_2-x_4)^2}\frac{\partial\Phi}{\partial x_1}(x_0,x_1,x_2)\\
&-\frac{2x_0^2+x_1^2+2x_2^2-4x_0x_2-x_0x_3-2x_1x_3+x_2x_3}{2(x_1-x_3)^2(x_2-x_4)}\frac{\partial\Phi}{\partial x_2}(x_0,x_1,x_2)\\
&+\frac{2x_0^2-x_1^2+2x_2^2-x_0x_1-4x_0x_2-x_1x_2}{2(x_1-x_3)(x_2-x_4)}\frac{\partial^2\Phi}{\partial x_1\partial x_2}(x_0,x_1,x_2)\\
&-\frac{2x_0^2+x_1^2+2x_4^2-x_0x_3-4x_0x_4-2x_1x_3+x_3x_4}{2(x_1-x_3)^2(x_2-x_4)^2}\Phi(x_0,x_1,x_4)\\
&+\frac{2x_0^2-x_1^2+2x_4^2-x_0x_1-4x_0x_4-x_1x_4}{2(x_1-x_3)(x_2-x_4)^2}\frac{\partial\Phi}{\partial x_1}(x_0,x_1,x_4)\\
&-\frac{2x_0^2-2x_2^2-x_3^2-x_0x_3-4x_0x_4+4x_2x_4+x_3x_4}{2(x_1-x_3)^2(x_2-x_4)^2}\Phi(x_0,x_3,x_2)\\
&+\frac{2x_0^2+2x_2^2-x_3^2-4x_0x_2-x_0x_3-x_2x_3}{2(x_1-x_3)^2(x_2-x_4)}\frac{\partial\Phi}{\partial x_2}(x_0,x_3,x_2)\\
&+\frac{2x_0^2-x_3^2+2x_4^2-x_0x_3-4x_2x_4-x_3x_4}{2(x_1-x_3)^2(x_2-x_4)^2}\Phi(x_0,x_3,x_4)\Big\}\,,
\end{aligned}
\tag{B6}
$$

$$
\begin{aligned}
\Xi_{_F}(x_0,x_1,x_2,x_3,x_4)=\frac{1}{4}\Big\{&\frac{1}{(x_1-x_3)(x_2-x_4)}\Big[\Phi(x_0,x_1,x_2)-\Phi(x_0,x_1,x_4)\\
&-\Phi(x_0,x_3,x_2)+\Phi(x_0,x_3,x_4)\Big]+\frac{x_0+x_1-x_2}{(x_1-x_3)(x_2-x_4)}\frac{\partial\Phi}{\partial x_0}(x_0,x_1,x_2)\\
&-\frac{x_0+x_1-x_4}{(x_1-x_3)(x_2-x_4)}\frac{\partial\Phi}{\partial x_0}(x_0,x_1,x_4)-\frac{x_0+x_3-x_2}{(x_1-x_3)(x_2-x_4)}\frac{\partial\Phi}{\partial x_0}(x_0,x_3,x_2)\\
&+\frac{x_0+x_3-x_4}{(x_1-x_3)(x_2-x_4)}\frac{\partial\Phi}{\partial x_0}(x_0,x_3,x_4)\Big\}\,,
\end{aligned}
\tag{B7}
$$

with $A_0=-\gamma_{_E}+\ln(4\pi x_{_\mu})$, $A_1=3-2\gamma_{_E}+2\ln\frac{4\pi}{x_{_\mu}}$. Here, $x_{_\mu}=\mu_{\rm NP}^2/m_{\rm w}^2$, and $\mu_{\rm NP}$ is the scale to integrate heavy particles out.

Defining $\lambda^2=x_0^2+x_1^2+x_2^2-2x_0x_1-2x_0x_2-2x_1x_2$, the two-loop vacuum function $\Phi(x_0,x_1,x_2)$ is written as

- $\lambda^2 > 0,\ \sqrt{x_1} + \sqrt{x_2} < \sqrt{x_0}$:

$$\begin{aligned}\Phi(x_0,x_1,x_2) &= (x_0+x_1-x_2)\ln x_0 \ln x_1 + (x_0-x_1+x_2)\ln x_0 \ln x_2 \\ &+(-x_0+x_1+x_2)\ln x_1 \ln x_2 + \lambda\Big\{2\ln\Big(\frac{x_0+x_1-x_2-\lambda}{2x_0}\Big) \\ &\times \ln\Big(\frac{x_0-x_1+x_2-\lambda}{2x_0}\Big) - \ln\frac{x_1}{x_0}\ln\frac{x_2}{x_0} - 2L_{i_2}\Big(\frac{x_0+x_1-x_2-\lambda}{2x_0}\Big) \\ &-2L_{i_2}\Big(\frac{x_0-x_1+x_2-\lambda}{2x_0}\Big) + \frac{\pi^2}{3}\Big\}\ , \end{aligned} \tag{B8}$$

where $L_{i_2}(x)$ is the spence function;

- $\lambda^2 > 0,\ \sqrt{x_0} + \sqrt{x_2} < \sqrt{x_1}$:

$$\Phi(x_0,x_1,x_2) = \text{Eq.(B8)}(x_0 \leftrightarrow x_1)\ ; \tag{B9}$$

- $\lambda^2 > 0,\ \sqrt{x_0} + \sqrt{x_1} < \sqrt{x_2}$:

$$\Phi(x_0,x_1,x_2) = \text{Eq.(B8)}(x_0 \leftrightarrow x_2)\ ; \tag{B10}$$

- $\lambda^2 < 0$:

$$\begin{aligned}\Phi(x_0,x_1,x_2) &= (x_0+x_1-x_2)\ln x_0 \ln x_1 + (x_0-x_1+x_2)\ln x_0 \ln x_2 \\ &+(-x_0+x_1+x_2)\ln x_1 \ln x_2 - 2\sqrt{|\lambda^2|}\Big\{Cl_2\Big(2\arccos(\frac{-x_0+x_1+x_2}{2\sqrt{x_1x_2}})\Big) \\ &+Cl_2\Big(2\arccos(\frac{x_0-x_1+x_2}{2\sqrt{x_0x_2}})\Big) + Cl_2\Big(2\arccos(\frac{x_0+x_1-x_2}{2\sqrt{x_0x_1}})\Big)\Big\}\ , \end{aligned} \tag{B11}$$

where $Cl_2(x)$ denotes the Clausen function.

---

[1] E. P. Shabalin, Yad. Fiz. **28**, 151(1978); Sov. J. Nucl. Phys. **28**, 75(1978).

[2] I. S. Alatrev *et. al.*, Phys. Lett. B **276**, 242(1992); K. F. Smith *et. al.*, Phys. Lett. B **234**, 191(1990).

[3] J. Ellis, S. Ferrara, and D. V. Nanopoulos, Phys. Lett. B. **114**, 231(1982); W. Buchmuller and D. Wyler, *ibid.* **121**, 321(1983); J. Polchinski and M. B. Wise, *ibid.* **125**, 393(1983).

[4] P. Nath, Phys. Rev. Lett. **66**, 2565(1991); Y. Kizukuri and N. Oshimo, Phys. Rev. D. **46**, 3025(1992); **45**, 1806(1992).

[5] T. Ibrahim, P. Nath, Phys. Rev. D. **58**, 111301(1998); M. Brhlik, G. J. Good, G. L. Kane, *ibid.* **59**, 115004(1999).

[6] D. Chang, W. Y. Keung, A. Pilaftsis, Phys. Rev. Lett. **82**, 900(1999); **83**, 3972(1999)(E); A. Pilaftsis, Phys. Lett. B. **471**, 174(1999); Nucl. Phys. B. **644**, 263(2002); D. Chang, W. F. Chang, and W. F. Keung, Phys. Lett. B. **478**, 239(2000); T. F. Feng, T. Huang, X. Q. Li, S. M. Zhao, and X. M. Zhang, Phys. Rev. D. **68**, 016004(2003).

[7] T. Ibrahim, P. Nath, Phys. Lett. B. **418**, 98(1998); J. Dai, H. Dykstra, R. G. Leigh, S. Paban, D. A. Dicus, Phys. Lett. B. **237**, 216(1990).

[8] Tai-Fu Feng, Phys. Rev. D **70**, 096012(2004) (hep-ph/0405192).

[9] A. I. Davydychev and J. B. Tausk, Nucl. Phys. B. **397**, 123(1993).

[10] J. Dai, H. Dykstra, R. G. Leigh, S. Paban, and D. A. Dicus, Phys. Lett. B. **237**, 216(1990); D. A. Dicus, Phys. Rev. D. **41**, 999(1990).

[11] R. Arnowitt, J. Lopez, and D. V. Nanopoulos, Phys. Rev. D. **42**, 2423(1990); R. Arnowitt, M. Duff and K. Stelle, *ibid.* **43**, 3085(1991).

[12] A. Manohar, and H. Georgi, Nucl. Phys. B. **234**, 189(1984).

[13] A. Pilaftsis, Phys. Rev. **D58**, 096010(1998); Phys. Lett. **B435**, 88(1998); A. Pilaftsis, C. E. M. Wagner, Nucl. Phys. **B533**, 3(1999); M. Carena, J. Ellis, A. Pilaftsis, C. E. M. Wagner, *ibid.* **586**, 92(2000); *ibid.* **625**, 345(2002).